

**Charles University**

**Faculty of Science**

Study programme: Cellular Biology

Branch of study: Cellular Biology



**Bc. Michal Kněžů**

Úloha jednotlivých aminokyselinových zbytků první  
transmembránové domény v deaktivaci P2X7 receptoru

Role of individual amino acid residues in the first transmembrane  
domain in deactivation of P2X7 receptor

Diploma thesis

Supervisor: RNDr Hana Zemková, CSc.

Praha, 2023

## **Prohlášení:**

Prohlašuji, že jsem závěrečnou práci zpracoval samostatně, pod vedením školitelky RNDr. Hany Zemkové, CSc. na jejím pracovišti na Fyziologickém ústavě Akademie věd České republiky, a že jsem řádně uvedl všechny použité informační zdroje a literaturu. Tato práce ani její podstatná část nebyla předložena k získání jiného nebo stejného akademického titulu.

V Praze 4. ledna 2023,

.....

Michal Kněžů

**Poděkování:**

Rád bych poděkoval své školitelce RNDr Haně Zemkové, CSc a členům jejího týmu za cenné vhledy a dobré rady týkající se mé práce. Dále bych také rád poděkoval své rodině, kamarádům a blízkým.

## **Abstrakt**

P2X7 receptor je trimerní ligandem otevíraný iontový kanál, aktivovaný extracelulárním ATP. Tento receptor je exprimovaný v mnoha tkáních a buněčných typech, jako jsou například gliové buňky, buňky imunitního systému, různé epitely a spermie, a hraje roli v mnoha buněčných a fyziologických procesech, jako například fagocytóza, regulace metabolismu nebo apoptóza. Podjednotka P2X7 receptoru se sestává z intracelulárního N- a C-konce, dvou transmembránových domén (TM1 a TM2) a velké extracelulární ligand vazebné domény. P2X7 má nízkou sensitivitu pro svůj přirozený ligand, avšak jeho dlouhá nebo opakovaná aplikace sensitivitu k agonistovi zvyšuje spolu s amplitudou proudové odpovědi receptoru. Aktivace P2X7 receptoru je také spojena s akumulací velkých organických kationtů, například fluorescentního barviva ethidium bromidu. Sensitizace receptoru je spojena s prodloužením deaktivace, jejíž mechanismus nebyl dosud zcela objasněn, a která může být měřena jako pokles proudu při odmytí agonisty. Tato práce se zabývá rolí jednotlivých aminokyselin v TM1 v kinetice deaktivace naivního a sensitizovaného P2X7 receptoru. Elektrofyziologická hole-cell patch clamp metoda byla použita k zaznamenání agonistou stimulovaného proudu a jeho poklesu u divokého typu P2X7 (P2X7-WT) a alaninových nebo leucinových mutantů TM1. U mutací, které výrazně pozměnily kinetiku deaktivace, byla také tudována jejich schopnost regulovat akumulaci ethidium bromidu. Konkrétně u Gly27Ala, Trp31Ala, Leu33Ala, Thr36Ala a Val41Ala byla pozorovaná změna v deaktivaci naivní odpovědi oproti P2X7-WT, přičemž všechny, kromě Thr36Ala, se také lišily v sensitizované odpovědi, která se navíc změnila u Phe38Ala. Změna v akumulaci ethidium bromidu byla pozorována u všech zmíněných mutací s výjimkou Thr36Ala. Model potkaního P2X7 receptoru odhalil, že Trp31, Leu3 a Val41 jsou důležité pro interakci TM1 a TM2 anebo interakci s lipidy a lipofilními molekulami v membráně. Tato práce identifikovala aminokyseliny v TM1, které regulují kinetiku deaktivace P2X7 receptoru a ovlivňují jeho schopnost akumulovat ethidium bromid.

## **Klíčová slova:**

P2X7 receptor, extracelulární ATP, purinergní signalizace, deaktivace receptoru, transmembránová doména

## **Abstract**

P2X7 receptor is trimeric ligand-gated ion channel activated by extracellular ATP. This receptor is expressed in various tissues and cell types, such as glial cells, immune system cells or Schwann cells, different epithelial tissues and sperm cells, and is involved in many cellular physiological processes such as metabolism regulation, phagocytosis or apoptosis. The P2X7 subunit is composed of intracellular N- and C-termini, two transmembrane domains (TM1 and TM2) and a large extracellular ligand-binding domain. P2X7 has low sensitivity for its natural agonist, but prolonged or repeated applications lead to its sensitization and increase in current amplitude. Activation of P2X7 receptor is also known to induce uptake of large organic ions, such as fluorescent dye ethidium bromide. Receptor sensitization is accompanied by prolongation deactivation, mechanism of which is still unknown, that can be measured as current decay evoked by washout of agonist. This work explores the role of individual TM1 residues in deactivation kinetics of the receptor both in naïve and sensitized states. Electrophysiological whole-cell patch clamp method was used to record agonist-stimulated membrane current and its decay of wildtype P2X7 receptor (P2X7-WT) and TM1 alanine or leucine mutants. Mutations that were found to impair or change receptor deactivation kinetics were also tested for their ability to regulate ethidium bromide uptake function of receptor. In particular, Gly27Ala, Trp31Ala, Leu33Ala, Thr36Ala, and Val41Ala were observed to differ in their deactivation kinetics in naïve state compared to P2X7-WT, and all but one (Thr36Ala) differed also in sensitized state, that was also changed in Phe38Ala. Impairment in ethidium bromide uptake was observed in all of these mutations except Thr36Ala. A model of rat P2X7 revealed that residues Trp31, Leu33 and Val41A are important for TM1 and TM2 interaction and/or for interaction with lipids and lipophilic molecules in the membrane. This work indicates that numerous residues in the TM1 regulate P2X7 deactivation kinetics that determine dye uptake function of this receptor.

## **Keywords:**

P2X7 receptor, extracellular ATP, purinergic signaling, receptor deactivation, transmembrane domain

## Abbreviations used

$\alpha\beta$ -meATP	$\alpha,\beta$ -Methyleneadenosine 5'-triphosphate
ADP	Adenosine-5'-diphosphate
AMP	Adenosine-5'-monophosphate
ATP	Adenosine-5'-triphosphate
BzATP	3'-O-(4-Benzoyl)benzoyladenosine 5'-triphosphate
cAMP	Cyclic adenosine monophosphate
Cryo-EM	Cryogenic electron microscopy
GDP	Guanosine-5'-diphosphate
HEK293T	Human embryonic kidney cells 293T
LPS	Lipopolysaccharide
NMDG	N-methyl-D-glucamine
PPADS	Pyridoxal phosphate-6-azophenyl-2',4'-disulfonic acid
P2X	Ionotropic purinergic receptor
P2Y	Metabotropic purinergic receptor
TM1	Transmembrane domain 1
TM2	Transmembrane domain 2
rP2X7	Rat P2X7 receptor
UDP	Uridine-5'-diphosphate
UTP	Uridine-5'-triphosphate
zfp2X4	P2X4 receptor from zebrafish ( <i>danio rerio</i> )

## Amino acids

Alanine	Ala	A
Arginine	Arg	R
Asparagine	Asn	N
Aspartate	Asp	D
Cysteine	Cys	C
Glutamate	Glu	E
Glutamine	Gln	Q
Glycine	Gly	G
Histidine	His	H
Isoleucine	Ile	I
Leucine	Leu	L
Lysine	Lys	K
Methionine	Met	M
Phenylalanine	Phe	F
Proline	Pro	P
Serine	Ser	S
Threonine	Thr	T
Tryptophane	Trp	W
Tyrosine	Tyr	Y
Valine	Val	V

# Contents

1. Introduction.....	1
1.1. Purinergic signaling:.....	1
1.2. P2X receptors:.....	3
1.2.1. P2X1 receptors:.....	4
1.2.2. P2X2 receptors:.....	4
1.2.3. P2X3 receptors:.....	4
1.2.4. P2X4 receptors:.....	5
1.2.5. P2X5 receptors:.....	5
1.2.6. P2X6 receptors:.....	6
1.2.7. P2X7 receptors:.....	6
1.3. Molecular structure and function of P2X receptors:.....	8
1.3.1. ATP binding site in P2X receptors:.....	10
1.3.2. P2X receptor channel opening mechanism and ion passage:.....	12
1.3.3. Role of TM1 domain in P2X receptor function:.....	15
1.4. Unique features of P2X7 receptor:.....	16
1.4.1. C-cys anchor:.....	17
1.4.2. Lipid moiety bound between TM1 and TM2 domains:.....	18
1.4.3. Cytoplasmic ballast:.....	18
1.4.4. Signaling motifs in P2X7 receptor:.....	19
1.4.5. P2X7 and phagocytosis:.....	21
1.4.6. P2X7 receptor's role in metabolism and mitochondria:.....	22
1.4.7. P2X7 receptor's role in phosphatidylserine exposure:.....	22
1.4.8. P2X7 in sperm:.....	23
1.4.9. Receptor sensitization and deactivation:.....	24
2. Aims of the study.....	25
3. Material and methods.....	26
3.1. Chemicals:.....	26
3.2. DNA constructs:.....	26
3.3. Cell culturing and transfection:.....	27
3.4. Patch clamp recordings:.....	27
3.5. Ethidium bromide uptake:.....	28
3.6. Calculations:.....	29
4. Results.....	30
4.1. Electrophysiological patch clamp recordings:.....	30
4.1.1. Deactivation kinetics of naïve P2X7-WT and TM1 mutants:.....	31

4.1.2. Deactivation kinetics of sensitized P2X7-WT and TM1 mutants: .....	36
4.2. Microfluorometric measurements:.....	38
5. Discussion .....	40
6. Conclusion .....	52
7. References .....	53

# 1.Introduction

## 1.1.Purinergic signaling:

Purinergic signaling as a concept was introduced by Geoffrey Burnstock in 1972. Adenosine-5'-triphosphate (ATP), for a long time considered to be only a source of cellular energy, is a key player in purinergic signaling (Geoffrey Burnstock, 1972). Extracellular ATP and its derivatives (adenosine-5'-diphosphate, ADP, and adenosine-5'-monophosphate, AMP), along with several other structurally similar compounds (such as uridine-5'-triphosphate, UTP, and uridine-5'-diphosphate, UDP), bind to their specific membrane receptors and stimulate many diverse signaling events (Abbracchio et al., 2009; Burnstock & Verkhratsky, 2012).

There are three types of receptors involved in purinergic signaling: P1 receptors, activated by adenosine; P2X receptors, activated by extracellular ATP; and P2Y receptors, activated by ATP, ADP, UTP, UDP, UDP glucose, UDP galactose, NAD<sup>+</sup> (Nicotinamide adenine dinucleotide) and NAADP<sup>+</sup> (Nicotinic acid adenine dinucleotide phosphate) (Abbracchio et al., 2009; Burnstock & Kennedy, 1985; von K ugelgen, 2019; Von Kugelgen & Wetter, 2000). These three types of purinergic receptors are structurally and functionally very diverse: while the P1 and P2Y receptors are metabotropic G-protein coupled receptors (GPCRs), the P2X receptors are ion channels, which may illustrate complexity of purinergic signaling (Fredholm et al., 1997).

Four subtypes of P1 receptors are known, all of which are metabotropic GPCRs with seven transmembrane domains. These are A<sub>1</sub>, A<sub>2A</sub>, A<sub>2B</sub> and A<sub>3</sub>. Two of them, A<sub>1</sub> and A<sub>3</sub>, are coupled with G<sub>i/o</sub> causing inhibition of adenylyate cyclase and reduced cAMP (cyclic adenosine monophosphate) synthesis. while A<sub>2A</sub> and A<sub>2B</sub> are coupled with G<sub>s</sub>, thus leading to activation of adenylyate cyclase and increased levels of cAMP (Fredholm et al., 2001; Libert et al., 1989; Schulte & Fredholm, 2003; Zhou et al., 1992). There are eight P2Y subtypes, which are divided into two major groups based upon the genetic classification of the G-protein to which they couple. P2Y<sub>1</sub>, P2Y<sub>2</sub>, P2Y<sub>4</sub>, P2Y<sub>6</sub> and P2Y<sub>11</sub> couple G<sub>q</sub>-proteins, and their stimulation leads to activation of phospholipase C and Ca<sup>2+</sup> release from intracellular stores. Receptors P2Y<sub>12</sub>, P2Y<sub>13</sub> and P2Y<sub>14</sub> couple G<sub>i/o</sub> proteins. P2Y<sub>11</sub> has also been found to couple G<sub>s</sub>-proteins. The third type of the purinergic receptors are P2X receptors, trimeric ion channels activated by extracellular ATP. There are seven subtypes (P2X<sub>1-7</sub>) of these receptors (Burnstock & Kennedy, 1985; Khakh et al., 2001), all of which will be briefly discussed later in a separate

chapter.

There are several ways, in which ATP or other ligands of purinergic receptors enter the extracellular space, where these molecules might activate purinergic receptors. The first and the most obvious one is cell damage (Vénéreau, Ceriotti, & Bianchi, 2015). When cell membrane is damaged, it allows for cytoplasmic contents of the cell, including ATP and similar compounds, to escape out of the cell into extracellular space, where many of them may act as modulators of immune system response, for example (Lazarowski, Boucher, & Harden, 2003).

Other way in which ATP can leave the intracellular space is through channels such as pannexins or connexins, that poses the ability to transport large molecules (Anselmi et al., 2008; Velasquez & Eugenin, 2014). There are also nucleotide transporters that can pump ATP into extracellular space. One of such transporter is vesicle nucleotide transporter, also known as VNUT (Vesicular nucleotide transporter), that is known to transfer ATP into lysosomes, endolysosomes and synaptic vesicles, which may later be fused with the cell membrane (Sawada et al., 2008). This is for example known to occur in lungs, where P2X4 is located in the membrane of lysosome itself and oriented to its lumen. These receptors are inhibited by low lysosomal pH, but once the organelle fuses with the cell membrane, the pH rises, which allows ATP, that was contained within the lysosome, to activate these P2X4 receptors, causing a localized signal in proximity to the fusion site (Miklavc, Thompson, & Frick, 2013). Finally, ATP is also released by regulated exocytosis of synaptic vesicles or secretory granules, along with release of neurotransmitters and hormones, respectively (Pankratov et al., 2006).

Once ATP or other ligands leave the cell, they become a substrate for many extracellularly located ectonucleotidases, which quickly digest these compounds. Among ectonucleotidases are ectonucleoside triphosphate diphosphohydrolases, alkaline phosphatases, phosphodiesterases, ectonucleoside pyrophosphatases and ecto-5'-nucleotidases, for example. These enzymes are capable of quick hydrolysis of ATP into ADP, AMP and adenosine. This serves two purposes: firstly, the rate of ATP hydrolysis allows control of the duration and strength of the P2X-mediated signal. Secondly, ATP metabolites act as ligands for other purinergic receptors, that are activating gradually cascade of purinergic signaling. In addition to ectonucleotidases, there are also other enzymes in the extracellular space, that are affecting purinergic signaling. These enzymes are generally kinases, such as adenylyl kinases or ectonucleoside kinases, that catalyze similar reactions as mentioned above, but in the opposite way. They are turning transformation of adenosine into

AMP, ADP and finally ATP, thus increasing the complexity to the purinergic signaling system, reviewed in (Abbracchio et al., 2009; Dwyer, Kishore, & Robson, 2020).

## 1.2. P2X receptors:

There are seven subtypes of P2X receptors (P2X1-7) in mammals. All of these subtypes are cationic channels permeable to  $\text{Na}^+$ ,  $\text{K}^+$  and  $\text{Ca}^{2+}$ . They are composed of three subunits, forming homotrimers or heterotrimers. All P2X are activated by extracellular ATP, but exhibit different biophysical and pharmacological properties (Nicke et al., 1998; North, 2002). Particularly, P2X subtypes differ in the rate of desensitization (Fig.1.1), sensitivity to agonists, antagonists and allosteric modulators, and ion permeability (North, 2002).

The P2X channels widely differ in physiological roles they serve and in their expression profiles in various tissues and cell types. A short introductory information about these subtypes will now be given in the following chapters, except P2X7 that will be introduced in more details.

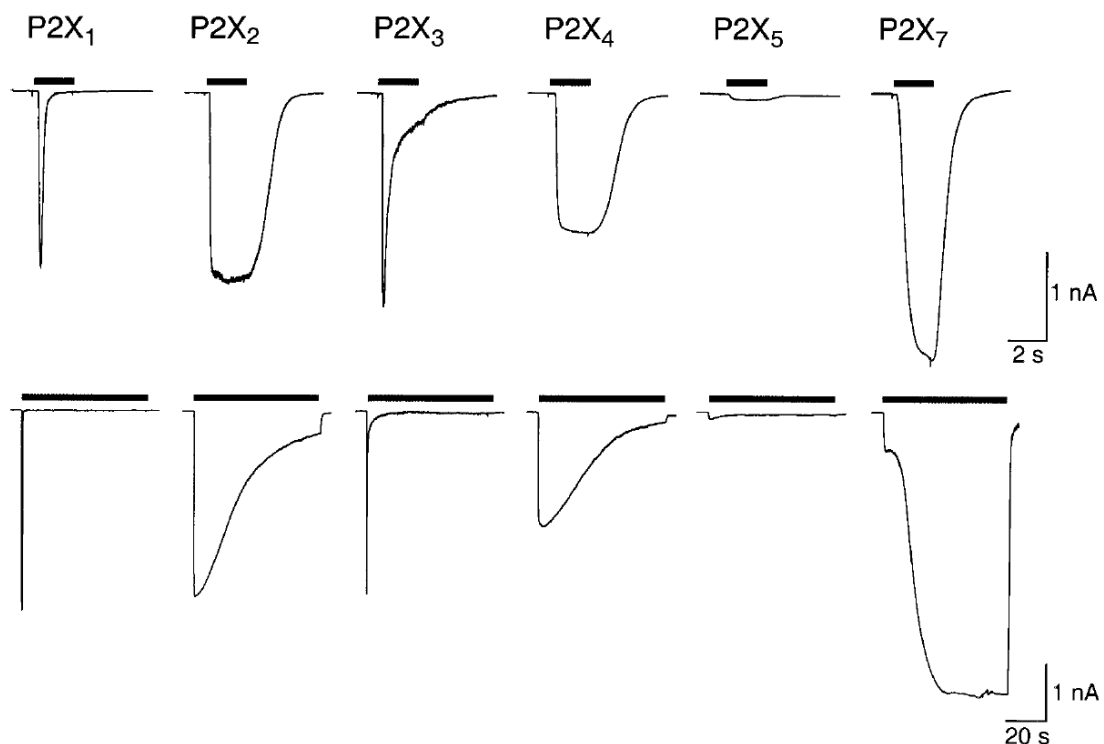


Figure 1.1: Depiction of transmembrane current mediated by P2X<sub>1</sub>, P2X<sub>2</sub>, P2X<sub>3</sub>, P2X<sub>4</sub>, P2X<sub>5</sub> and P2X<sub>7</sub> receptors after short (upper) and long (bottom) application of 30 μM ATP (1 mM ATP for P2X<sub>7</sub>). Figure was taken from (North, 2002).

### 1.2.1. P2X1 receptors:

P2X1 receptors are expressed namely in urinary bladder and vas deferens, where they are known to have a role in contraction of smooth muscles, or in neutrophil chemotaxis or thromboinflammation (Lecut et al., 2009; North, 2002; Oury & Wéra, 2021). P2X1 can be activated by its natural ligand, such as ATP, but also by synthetic ligands such as  $\alpha\beta$ -meATP, ( $\alpha,\beta$ -Methyleneadenosine 5'-triphosphate) which acts in concentration similar to that of ATP, or BzATP (3'-O-(4-Benzoyl)benzoyladeniosine 5'-triphosphate) which acts at higher concentrations (Bianchi et al., 1999; North, 2002). There are several non-specific inhibitors of P2X1, such as suramin or PPADS, yet more selective and specific antagonist have also been found. P2X1 desensitizes more quickly compared to other P2X subtypes (Fig. 1.1). It is cation selective channel with a low permeability for large organic cations, such as N-methyl D-glucamine (NMDG) (Evans et al., 1996; North, 2002).

### 1.2.2. P2X2 receptors:

P2X2 receptors are highly expressed in different regions of the brain, where they are present in different splice variants. They are known to have function in inflammatory and neuropathic pain, and sense of taste (Kaan et al., 2010; Lynch et al., 1999; North, 2002; Vulchanova et al., 1997). P2X2 is considered to be a non-desensitizing receptor channel selectively permeable to cations and large positively charged organic compounds, such as previously mentioned NMDG (Lynch et al., 1999; North, 2002). Potential structural reasons for the non-desensitizing character of this receptor were examined in 3D structure studies (Mansoor et al., 2016) and are discussed latter (section 1.3.). P2X2 can be inhibited by PPADS and suramin (Zhong et al., 1998), up to date, no P2X2-specific inhibitor has been found.

### 1.2.3. P2X3 receptors:

P2X3 receptors are known to form heteromeric channels with P2X2 receptors, and to play a crucial role in pain signaling (Ding et al., 2017; Kaan et al., 2010; North, 2004). This receptor subtype is also involved in taste and temperature sensing or bladder contraction (Finger et al., 2005; Khmyz et al., 2008). It is a fast desensitizing receptor, almost like P2X1, and its recovery from desensitization can last for more than 15 minutes. It can be activated by submicromolar concentrations of ATP or  $\alpha\beta$ -meATP, and is inhibited by suramin, PPADS and TNP-ATP (2'-(or-3')-O-(Trinitrophenyl) Adenosine 5'-Triphosphate), just like P2X1 (Garcia-Guzman, Stühmer, & Soto, 1997; Virginio, North, & Surprenant, 1998). Specific

inhibitors of P2X3 are also known, for example Gefapixant or Sivopixant are currently clinically tested as perspective drugs for curing cough (Cui et al., 2022; Niimi et al., 2022).

#### 1.2.4. P2X4 receptors:

P2X4 receptors can be found in different tissues and organs. They are highly expressed in hypothalamus, peripheral ganglion, cerebellum, hippocampus, supraoptic nucleus or glial cells or gastrointestinal tract (Bhattacharya et al., 2013; Buell et al., 1996; G. Burnstock & Kennedy, 2011; Kanellopoulos et al., 2021; Luo et al., 2006; Montilla et al., 2020; North, 2002; Shibuya et al., 1999; Vavra, Bhattacharya, & Zemkova, 2011; Wheeler-Schilling et al., 2001). As mentioned above, P2X4 is also located in endolysosomes (Murrell-Lagnado, 2018). P2X4 receptor can be activated by ATP, but not by  $\alpha\beta$ -meATP, which can be used to distinguish P2X4 from other P2X subtypes. P2X4 can be selectively allosterically potentiated by ivermectin. P2X4 action is inhibited by acidic environment and by suramin and PPADS, even though the effect of these two compounds is lower compared to that observed for other P2X receptors. P2X4 is cation selective channel that also permeable to large organic cations, such as NMDG. It is a moderately desensitizing channel (Fig. 1.1) (North, 2002; Stoop, Surprenant, & North, 1997; Wildman, King, & Burnstock, 1999; Xiong et al., 1999). It is known to form heteromeric receptors with P2X6 and P2X7, however, no specific features of these heteromers have been discovered up to date, and it is supposed that these receptors attain functional properties of the subtype with more subunits present in heterotrimeric structure (Schneider et al., 2017).

#### 1.2.5. P2X5 receptors:

P2X5 receptors are expressed in many parts of central nervous system of mice, such as olfactory bulb, supraoptic nucleus, ventrolateral nucleus of thalamus, pontine nuclei and many more. It is known to have very low current amplitude compared to that of other P2X subtypes (Fig. 1.1). P2X5 agonists are ATP,  $\alpha\beta$ -meATP and BzATP. It can be inhibited, similarly to other subtypes, by suramin or PPADS application. The channel is known to be permeable to NMDG and also chloride ions (Collo et al., 1996; Garcia-Guzman, Soto, Laube, & Stühmer, 1996; Lê, Boué-Grabot, Archambault, & Séguéla, 1999; North, 2002). P2X5 is also known to form heteromeric structures with P2X1, P2X2 and P2X4 subtypes, and the P2X2/P2X5 heteromers were reported to have characteristics similar to that of P2X7 receptors (Compan et al., 2012).

#### 1.2.6. P2X6 receptors:

P2X6 receptors are called “silent” receptors, since they are not known to elicit any current when expressed on their own in transfected cells. However, when expressed together with some other P2X subtype, a response different from the coexpressed subunit can be obtained. P2X6 is thought to form heteromeric channels with P2X2 and P2X4. It is known to be expressed in central nervous system and gastrointestinal tract (Collo et al., 1996; King et al., 2000; Lê, Babinski, & Séguéla, 1998; North, 2002).

#### 1.2.7. P2X7 receptors:

P2X7 receptors, originally dubbed as P2Z receptors, are also present in various tissues and cell types (Fredholm et al., 1997). In the central nervous system, P2X7 is present in astrocytes, various glial cells, Schwann cells, T-cells, macrophages and it is known to play important role in inflammation, cell death and cancer (Kopp et al., 2019; Miras-Portugal et al., 2017).

The P2X7 gene contains 13 exons and up to 10 splicing variants are known or theorized to be expressed, some varying significantly in their function (Andrejew et al., 2020). It is also known, that different P2X7 splice variants have different characteristics, some being more or less sensitive to the agonist, while other not being functional at all. Activity of different variants also leads to different signaling outcomes (Cheewatrakoolpong et al., 2005; De Salis et al., 2022). For example, two functionally different splice variants are known as P2X7A and P2X7B. P2X7A is composed of the whole known primary structure of the receptor, however P2X7B is truncated compared to P2X7A. P2X7B is shorter by about 231 amino acids on its C-terminus, which otherwise, as will be discussed later, harbors several important structural and functional motifs. These two splice variants differ functionally, as the C-terminus is important for the passage of large cations (Adinolfi et al., 2010; Cheewatrakoolpong et al., 2005; Di Virgilio, Schmalzing, & Markwardt, 2018). Long C – terminus, specific for P2X7 receptor of P2X7A splice variant, contains many important structural and functional motifs, which will be discussed later (section 1.4.). These motifs suggest, that P2X7A’s long C-terminus is an important signaling hub (Kopp et al., 2019; McCarthy, Yoshioka, & Mansoor, 2019).

Natural ligand for P2X7 is extracellular ATP. P2X7 sensitivity to ATP is very low compared to other P2X, it can be activated only by high micromolar or low millimolar

concentrations of ATP. Selective P2X7 agonist is BzATP, synthetic analogue of ATP, which activates P2X7 at low micromolar concentrations (North, 2002; Surprenant et al., 1996).

However, there are also other possible pathways that may lead to P2X7 receptor activation apart from binding of ATP or BzATP. It has been reported, that amyloid- $\beta$ , cathelicidin and serum amyloid can directly open the P2X7 pore in cell endogenously expressing this receptor (Di Virgilio et al., 2018; Elssner et al., 2004; Niemi et al., 2011; Sanz et al., 2009). However, this stimulation could be also due to endogenous ATP released from treated cells, that would then in turn activate P2X7 receptors. It has also been shown that lipopolysaccharide, a bacterial toxin, leads to P2X7 sensitization if present in the intracellular space (Di Virgilio et al., 2018; Ferrari et al., 1997; Yang et al., 2015). Finally, an accumulation of Alu-RNA, a short RNA transcript of Alu elements, in cytoplasm is capable of opening P2X7 receptor channel without any known ATP stimulation (Fowler et al., 2014).

P2X7 can be inhibited by low pH and divalent cations, while being relatively insensitive to PPADS or suramin (North, 2002; Surprenant et al., 1996). However, new synthetic drugs were created and proposed to be effective P2X7 allosteric inhibitors, which are specific for this P2X subtype (Donnelly-Roberts et al., 2009; Honore et al., 2006; Michel et al., 2007; Michel, Chambers, & Walter, 2008; Michel, Clay, et al., 2008). P2X7 receptor is a cation selective channel exhibiting high permeability to calcium and is also permeable to large organic cations, such as NMDG, Yo-pro fluorescent dye or ethidium bromide (North, 2002; Surprenant et al., 1996; Virginio et al., 1999).

P2X7 receptor is involved in wide variety of cellular physiological and pathophysiological processes. C-terminus of P2X7 receptor harbors many signaling motifs thus making a possible signaling hub for a variety of intracellular signaling pathways (Kopp et al., 2019).

Among the phenomena in which the P2X7 is involved are for example neurodegenerative diseases such as Alzheimer's disease, Parkinson's disease and neuroinflammation. P2X7 receptor is known to induce the ability to phagocytose when expressed in HEK293 cell line (Gu et al., 2009). Its activity has also been connected to cell proliferation, apoptosis and membrane blebbing (North, 2002). Some studies have also linked P2X7 to metabolism and mitochondria, as it might seem that the receptor can also be present on this organelle and it was found, that low but sustained P2X7 activation can lead to upregulation of cellular metabolism and general increase in levels of ATP in the cell (Adinolfi et al., 2005; Sarti et al., 2021). Specific role of P2X7 in cellular physiological processes is later described in more detail (Sections 1.4.5. – 1.4.8.)

### **1.3. Molecular structure and function of P2X receptors:**

The P2X family defines a unique structure for ligand-gated ion channels. The primary structures of different P2X subunits vary in size, ranging from 384 amino acids to 595 amino acids, and the largest is P2X7 receptor, because of its long intracellular C-terminus. Each of the receptor subunit has two transmembrane structures (TM1 and TM2) with both the N- and C-terminus located intracellularly. The pairwise amino acid identity of transmembrane domain ranges from around 40% to 55% between subtypes. The P2X4 is the most similar to all other subtypes and P2X7 is the least identical to the other receptor subtypes, because of its aforementioned long C-terminus. The extracellular domain, extending from residue 51-329 for P2X2, makes up the bulk of the protein and has been shown to account for ATP binding (North, 2002).

Up to date, molecular structures have been solved for zebra fish P2X4 (zfP2X), human P2X3 (hP2X3) and panda P2X7 (pdP2X7) (Hattori & Gouaux, 2012; Karasawa & Kawate, 2016; Kawate et al., 2009; Mansoor et al., 2016; McCarthy et al., 2019). All these structures show that P2X contain intracellularly located N- and C-termini, two  $\alpha$ -helical transmembrane domains and, in between these domains, a large extracellular loop containing the ATP binding pocket. The first P2X structure that was solved was crystal structure of zfP2X4, published in 2009. This study revealed that the P2X monomer has a shape similar to that of dolphin with head, left and right flipper, dorsal fin, upper and lower body that all form the large extracellular loop, while the fluke is composed of both transmembrane domains. This study did not show structure of intracellular N- and C-termini, since the zfP2X4 construct was truncated in order to be more viable for crystallization (Kawate et al., 2009). In later years, more P2X structures were solved, either by X-ray crystallography (Hattori & Gouaux, 2012; Mansoor et al., 2016) or by cryo-EM (cryogenic electron microscopy) (McCarthy et al., 2019). Among these were hP2X3 and rP2X7 structures that revealed also details about intracellular N- and C-termini. The extracellular part and transmembrane domain of P2X receptors has a goblet-like shape with each subunit turning around the receptor axis, being held together by numerous interactions in between subunits' body domains (Fig. 1.2) (Hattori & Gouaux, 2012; Karasawa & Kawate, 2016; Kawate et al., 2009; Mansoor et al., 2016; McCarthy et al., 2019).

In the study on hP2X3 structure (Mansoor et al., 2016), the construct of P2X3 contained three mutated amino acids on its N-terminus that are normally present in the non-desensitizing P2X2 wildtype. These three mutations, Thr13Pro, Ser15Val and Val16Ile,

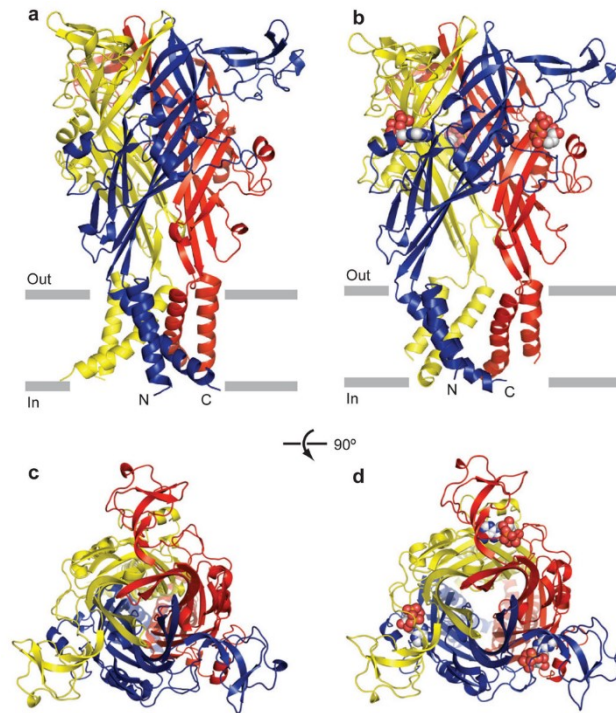


Figure 1.2: Depiction of zfpP2X4 receptor structure, resembling a goblet, viewed from side (a and b) and from above (c and d), in its closed state (a and c) and open state (b and d) (Taken and adjusted from (Hattori & Gouaux, 2012))

allowed discovery of novel feature in P2X called “cytoplasmic cap”. It is supposed that formation cytoplasmic cap is responsible for non-desensitizing character of the P2X3 construct. The cytoplasmic cap was observed only in the open state of the receptor but was unstructured in apo (closed) state of the receptor. It is therefore assumed that cytoplasmic cap is a dynamic structure that it is formed upon ligand binding. The authors of the study argue, that cytoplasmic cap probably functions as an anchor to the transmembrane domain helices, holding them in their open state conformation and thus keeping the receptor not desensitized (Fig. 1.3) (Mansoor et al., 2016).

Cytoplasmic cap and several new features in the intracellular part were also observed in cryo-EM structure of rat P2X7 (McCarthy et al., 2019). However, cytoplasmic cap seems to be present even in closed state in P2X7 receptor, not being a dynamic structure such as it is in the P2X3 construct structure or putatively in the P2X2 receptor. Cytoplasmic cap is composed of three  $\beta$  sheets. These  $\beta$  are formed by both N- and C-terminal strands of each subunit, where N-terminal strand of one subunit interacts with a C-terminal strand of the neighboring subunit (Mansoor et al., 2016; McCarthy et al., 2019).

In addition to the aforementioned cytoplasmic cap, two new structural features were discovered in the P2X7. The first is so called “cytoplasmic ballast”, which is a large globule-

like structure present on each of P2X7 subunits C-terminus, that is thought to be involved in

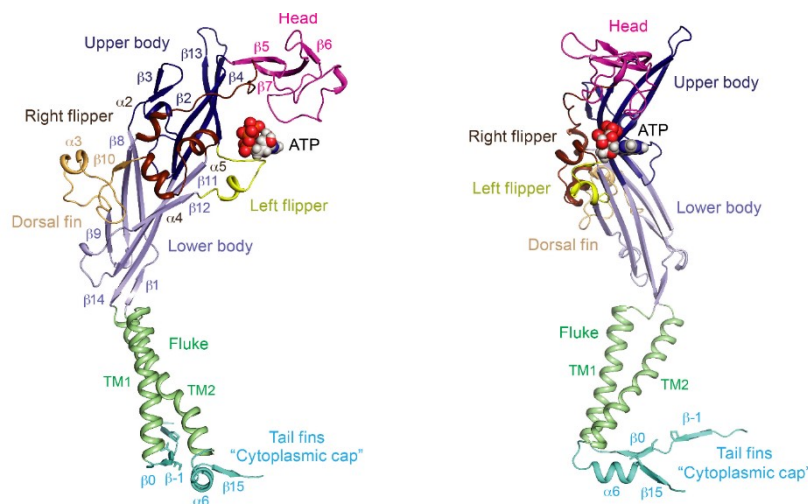


Figure 1.3: Depiction of hP2X3 receptor protomer structure from side and from two different angles with bound ATP. Strands that make up the cytoplasmic cap are located intracellularly and are highlighted in turquoise (taken and adjusted from (Mansoor et al., 2016)).

P2X7 intracellular signaling pathways. The second one is known as “C-cys anchor”, also present on each subunit, that can be palmitoylated and is important for anchoring the receptor in the membrane (McCarthy et al., 2019). All these P2X7-specific features will be later discussed in detail (sections 1.4.1. and 1.4.3.).

### 1.3.1. ATP binding site in P2X receptors:

The P2X crystal and cryo-EM structures have also shown striking similarities in key amino acid residues within ATP binding pocket of all P2X subtypes, along with a very specific way of ATP molecule binding and ligand-protein interaction, that is known only in P2X and aminoacyl synthetases of class II (Cavarelli et al., 1994; Hattori & Gouaux, 2012; Mansoor et al., 2016; McCarthy et al., 2019).

ATP binding pocket lies between P2X subunits, thus the trimeric receptor has three ATP binding pockets, and contains conserved positively charged amino acid residues that interact with the ligand molecule (Fig. 1.4).

These conserved residues, that lie in between upper body, lower body, head, left flipper and dorsal fin (Fig. 1.4) are: Lys 70, Lys72, Asn296, Lys316, Thr189, Leu191, Ile232, Leu217 and Lys293 (numbered according to the zfp2X4). The way in which ATP binds within the ATP binding pocket is very unusual. ATP is bound in “U” conformation which was only observed in aminoacyl synthetases of class II (Cavarelli et al., 1994; Hattori & Gouaux, 2012). In this conformation,  $\beta$  phosphate and  $\gamma$  phosphate are turned to be in proximity to the adenine, which

is in the anti-conformation to the ribose ring. This conformation allows ATP binding to the P2X via formation of hydrogen bonds and salt bonds between the ligand molecule and the aforementioned conserved polar and basic residues in the ATP binding site. With ATP bound in the ATP binding pocket, Lys70 amino group is located in the middle of the “U” shape of

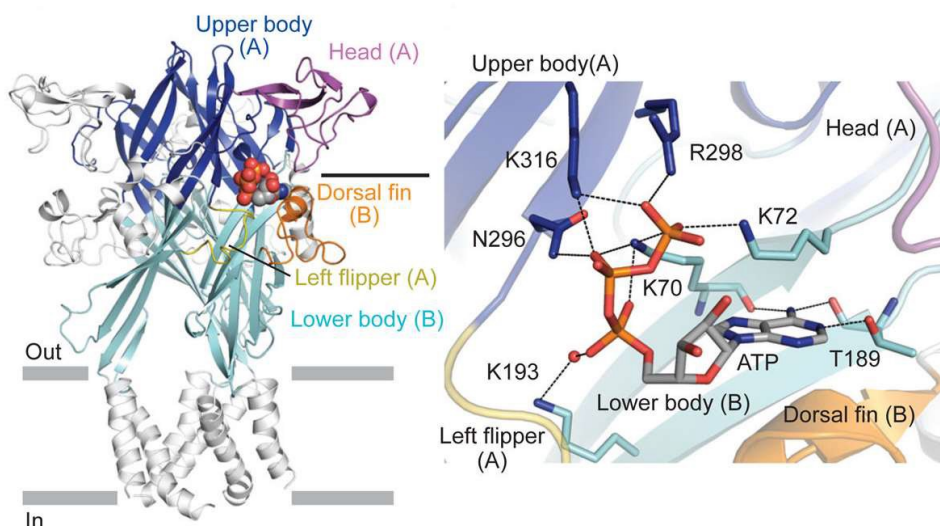


Figure 1.4: Depiction of ATP binding pocket and ATP bound in its “U” conformation in zfp2X4 receptor structure (taken and adjusted from (Hattori & Gouaux, 2012))

the ligand molecule and interacts with oxygen ions of all three phosphate groups of ATP.  $\beta$  phosphate group further interacts with Asn296 and Lys316 and  $\beta$  phosphate group interacts with Lys72, Arg298 and Lys316. The adenine base, buried deeply within the ATP binding pocket, is recognized by interactions with conserved amino acids Thr189, Lys70, Leu 191 and Ile 232. First two of these amino acids are highly conserved and are thought to be linked to the channel opening mechanisms. The ribose ring of ATP is recognized through its hydrophobic interaction with Leu 218 (Hattori & Gouaux, 2012).

P2X receptors do not recognize any other nucleotides as ligands because of specificity of these above-mentioned interactions. Lys70 interaction with  $\beta$  phosphate and  $\gamma$  phosphate groups is probably the reason for the inability of ADP and AMP to activate P2X, since these key interacting groups are missing in these compounds (Gever, Cockayne, Dillon, Burnstock, & Ford, 2006). Furthermore, other bases are of incorrect size or do not possess appropriate groups needed to interact with P2X. O2 and O3 of ligand’s ribose ring are exposed to solvent and it is thought that this interaction with solvent is important for the specificity as well (Bianchi et al., 1999; Hattori & Gouaux, 2012; Virginio et al., 1998). Although the amino acids within ATP binding site are highly conserved and the mechanism of binding is generally

very similar in all P2X, there are some differences between ligand binding in three receptors whose structure is known. The P2X3 contains two more amino acids within its ATP binding site, these are Phe174 and Ser275, that interact with the ligand (Mansoor et al., 2016). ATP binding pocket of P2X7 is much more narrow and therefore harder for ligand to access, which is thought to be the main reason for P2X7 lower sensitivity to ATP as compared with other P2X (Karasawa & Kawate, 2016).

### 1.3.2. P2X receptor channel opening mechanism and ion passage:

ATP binding stimulates notable structural changes and conformation shifts that allow for the ion channel opening and ion passage through the pore. Upon the ligand binding, dorsal fin moves upwards, toward the head domain, which leads to expulsion of the left flipper from the ATP binding pocket. Lower body domain is connected to dorsal fin and left flipper domains and therefore these changes lead to tension in the lower body domain and rotation of the receptor's subunits. The tension is then transferred onto the transmembrane helices (Fig. 1.3 and Fig. 1.5) (Hattori & Gouaux, 2012; Mansoor et al., 2016; McCarthy et al., 2019).

The TM2 lines the wall of the channel pore and acts as the channel gate, that is in direct contact with the hydrated ions that pass through the receptor. TM1 does not interact with the ions and is on the "outside" of the transmembrane part of the channel. It can interact with the membrane lipids and molecules and is known to have an allosteric effect on the ion passage, even though it is not in direct contact (Kawate et al., 2009). The tension transferred to TM2 helices causes them to rotate around their axis and the receptor axis and change their angle to the membrane. This creates an opening of the pore by movement similar to an iris opening. The gate of the channel lies roughly in the middle of TM2, and their rotation around their axis breaks apart interactions of amino acids in the gate area (Fig. 1.5) (Hattori & Gouaux, 2012).

In study on the P2X3 structure, novel details about the channel opening mechanism were discovered (Mansoor et al., 2016). The P2X3 open state structure was gained from the P2X3 construct with three mutations corresponding to the sequence of P2X2, as described previously. In this P2X3 construct, the helices were not only rotated around their axis and angled, but they were also slightly pulled from the membrane, thus the key gating amino acids were separated from each other by rotating and also by pulling TM2 domains apart from each other. The tension in the pulled TM2 helices caused partial change their secondary structure within a small area. The normally  $\alpha$  helical structure of these domains is turned into a  $3_{10}$

helical structure, with different groove depth, due to the tension in lower body domain and the cytoplasmic cap holding and anchoring ends of these helices firmly in the membrane (Mansoor et al., 2016).

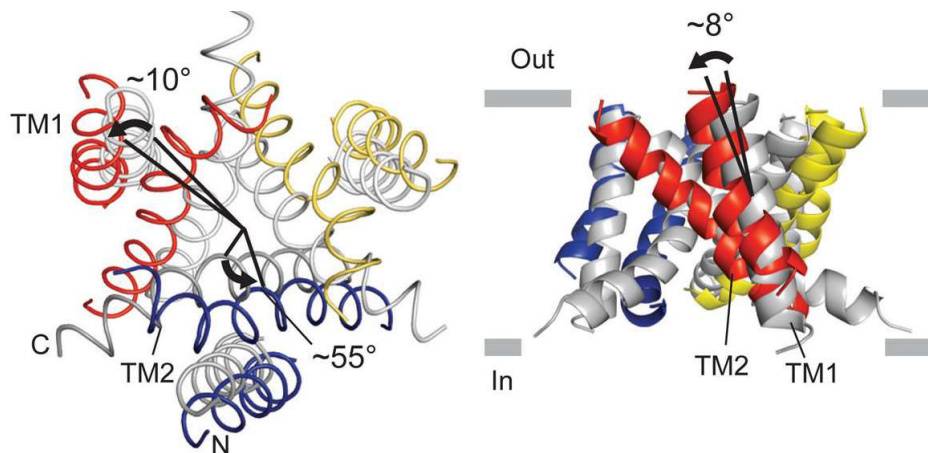


Figure 1.5: Depiction of shift and rotation of transmembrane helices in zfpP2X4 receptor structure viewed from cytoplasmic side of the membrane (left) and from side parallel to the membrane (right). Blue-, red- and yellow-colored helices correspond to open state of the channel (each color representing a subunit), while the grey helices represent closed state of the receptor.

Originally it was not well understood how the ions could pass through the P2X channel and it was suggested that the ions are passing through whole mass of the receptor, along its central axis, in between three subunits. There are several cavities, known as vestibules, along the P2X axis, which were originally thought to represent this pathway. However, upon closer inspection, it was found out, that even in the active state of the receptor with the ligand bound, there is not enough space along the axis in the middle of the receptor for the ions to fit through (Kawate et al., 2009). Crystallized constructs of zfpP2X4 in closed and open state with bound ligand (Hattori & Gouaux, 2012) revealed an alternative ion pathway. This pathway takes in account large fenestrations on sides of the trimer, that are located on the outer side of the membrane in close proximity to both transmembrane domains. These fenestrations, known as extracellular vestibule, are large enough (unlike the central openings along the axis) to allow for hydrated ion passage (Hattori & Gouaux, 2012). Upon receptor activation and channel opening, the ion can move through the extracellular vestibule which is enlarged. From here, ions move to the open channel gate within the membrane and to an intracellular vestibule, and then through intracellular fenestrations, which were discovered on P2X3, into the cytoplasm (Fig. 1.6) (Hattori & Gouaux, 2012; Mansoor et al., 2016).

The only part of the ion pathway, in which the ions actually move through the middle of the

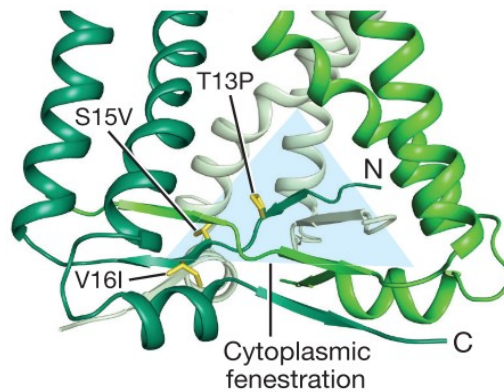


Figure 1.6: Depiction of cytoplasmic cap, formed in open state of hP2X3 receptor construct with key cap-forming mutations corresponding to non-desensitizing P2X2 receptor. Cytoplasmic fenestration, a part of ion passage pathway, is highlighted in light blue (taken and adjusted from (Mansoor et al., 2016)).

receptor along its central axis, is therefore the gate itself, localized in the middle of TM2 domains (Fig. 1.7) (Mansoor et al., 2016).

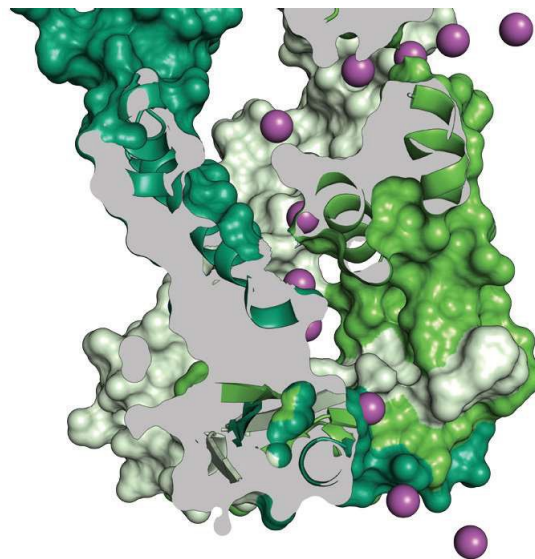


Figure 1.7: Depiction of ion passage pathway in hP2X3 structure, discovered by computer simulations. Ions pass through extracellular fenestrations to the channel itself and leave through intracellular fenestrations (taken and adjusted from (Mansoor et al., 2016))

It is important to note other vestibules in the body of the receptor. There are three such spaces in the extracellular part of the receptor and one, the intracellular vestibule, in the

intracellular part, located along the axis. Above the extracellular vestibule, a central vestibule is located (Hattori & Gouaux, 2012). The central vestibule is thought to play a role in concentrating ions near the extracellular vestibule via electrostatic interactions (Gonzales, Kawate, & Gouaux, 2009). Above the central vestibule is so called upper vestibule, which has so far unknown function (Hattori & Gouaux, 2012).

### 1.3.3. Role of TM1 domain in P2X receptor function:

Even though TM1 domain is not the one in direct contact with hydrated ions passing through the receptor gate, it serves many important roles in the receptor function (Kawate et al., 2009). This domain contains several conserved amino acids, whose residues seem to be crucial for receptor's correct function.

Functionally important are aromatic residues that are conserved in most of P2X receptors, with the exception of P2X7 (Haines et al., 2001; Jelínková et al., 2008; Li et al., 2004; Jindrichova et al., 2010). One such example is Tyr42 in P2X4, that when substituted by alanine, is known to dramatically change receptor behavior. Alanine mutation of this residue causes the P2X4 receptor to have considerably higher ATP sensitivity for both ATP and  $\alpha\beta$ -meATP and significantly elongated receptor deactivation. Substitution of this residue by residue with aromatic properties, such as phenylalanine or tryptophane, restores the original receptor function (Jindrichova et al., 2010). Yet this is not the only TM1 mutation in P2X4 that changes the receptor's sensitivity for ATP and its other characteristics, thus indicating the whole TM1 region as a crucial site for regulation of receptor's response and function (Jindrichova et al., 2010).

TM1 function is implied in many different manners. Based on zFP2X4 models, it was found out, that there are no extensive interaction between subunits in the transmembrane area of the receptor trimer in its open conformation and that, based on computer simulations, it seems unlikely for this receptor construct used for crystallization is properly functional, probably because missing their intracellular termini (Heymann et al., 2013; Kawate et al., 2009). However, this study mainly focused on the interactions between TM1 and TM2, that seems to be important for the channel gate stability and function. These experiments led to creation of constructs with metal bridges forming residues, substituting some of the original TM1 and TM2 amino acids, that in the presence of  $\text{Cd}^{2+}$  ions showed increased receptor potentiation. Based on these simulated cadmium metal bridges, the authors suggested a new reviewed model of transmembrane domains and interactions between TM1 and TM2 within

each subunit, reinforcing the importance of TM1 in transmembrane area stabilization (Heymann et al., 2013).

Another important function of TM1 domain of P2X is its role in binding of allosteric modulator (Zemkova et al., 2014). Ivermectin effectively binds to P2X4 and affects its behavior (Khakh et al., 1999). This allosteric regulator of P2X4 and other ion channels, such as glutamate-gated channels, GABA $\gamma$ -aminobutyric acid) receptors or glycine receptors, is a large lipophilic molecule, used in primarily in veterinary medicine as an effective drug for treatment of parasitic helminth infections (Cully et al., 1994; Krůšek & Zemková, 1994; Shan, Haddrill, & Lynch, 2001; Zemkova et al., 2014). Ivermectin was found to bind to several non-polar residues of amino acids in the upper part of TM1 domain as well as few residues on TM2 domain, thus the molecule seems to interact with both transmembrane domains (Zemkova et al., 2014).

#### 1.4. Unique features of P2X7 receptor:

In study published in 2019, the full-length P2X7 structure was solved using cryo-EM (McCarthy et al., 2019) (Fig. 1.8). This structure revealed several novel features important for P2X7 function. Apart from previously observed cytoplasmic cap (Mansoor et al., 2016), C-cys anchor and

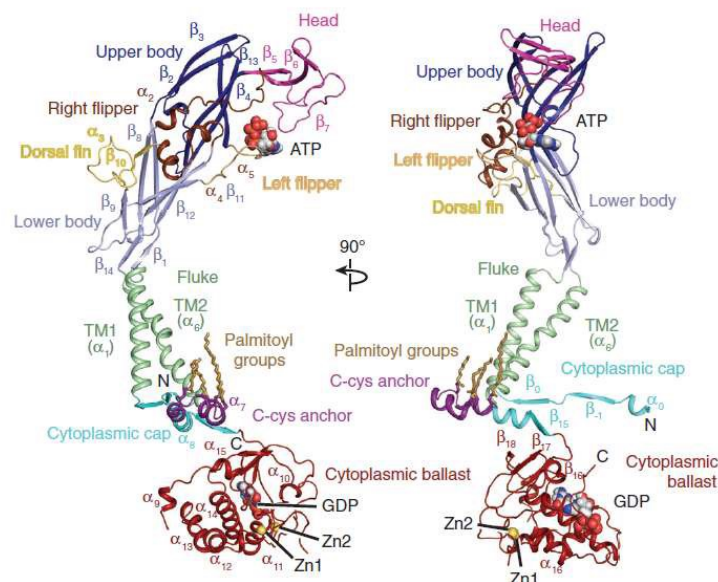


Figure 1.8: Depiction of rP2X7 protomer whole-length structure in open state with bound ATP. The transmembrane and extracellular loop are reminiscent of other known P2X receptor structures, while novel structural features, C-cys anchor cytoplasmic ballast were not observed in other P2X receptor structures (Taken and adjusted from (McCarthy et al., 2019)).

cytoplasmic ballast was discovered (Fig. 1.9). Additionally, a lipid moiety was also found to be bound between the P2X7 receptor's TM1 and TM2 domains (McCarthy et al., 2019).

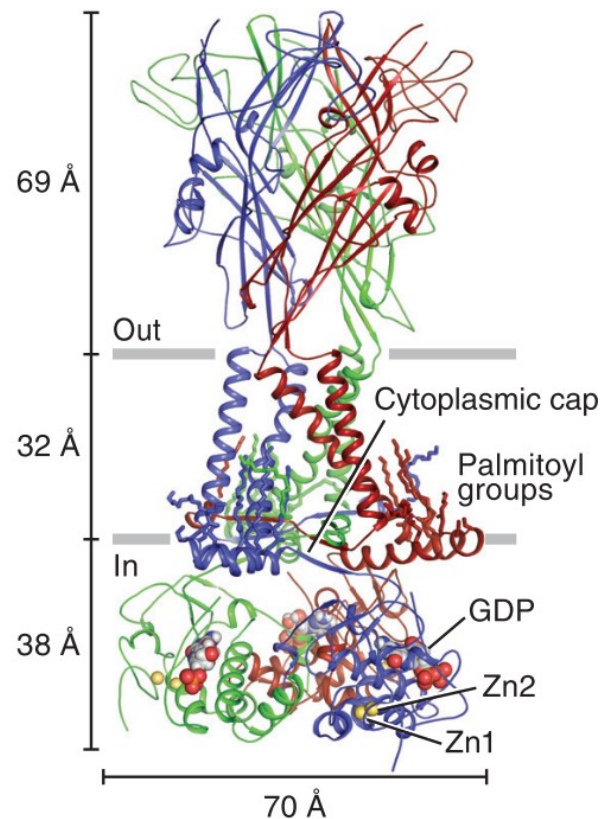


Figure 1.9: Depiction of full-length rP2X7 trimer with cytoplasmic ballast and other receptor-specific structures (taken and adjusted from (McCarthy et al., 2019)).

#### 1.4.1. C-cys anchor:

C-cys anchor is a structural feature present on each individual P2X7 receptor subunits (Fig. 1.10). It consists of a 21 amino acid long chain, that contains several cysteine residues. This chain, located just after TM2 domain, forms a loop in the inner side of the membrane. This loop is mostly of alpha-helical structure and lies “flatly” on the inner membrane surface. The cysteine residues on this feature, namely C362, Cys363, Cys374 and Cys377, were found to have palmitoyl groups attached to them. Ser360 present on the C-cys anchor is also known to be palmitoylated as well as yet another cysteine residue, Cys4, which however is far away from the C-cys anchor and is not considered a part of it. These palmitoyl groups were found to be facing upwards into the membrane, thus providing a large number of interactions with the membrane itself (McCarthy et al., 2019). Authors of the 3D structure found a connection between C-cys anchor and cytoplasmic cap and argue, that the purpose the C-cys anchor serves, is to maintain the presence of the cytoplasmic cap and thus disallow for receptor

desensitization. If these cysteine residues are mutated to alanine or otherwise truncated, the receptor can be then desensitized(Allsopp & Evans, 2015; McCarthy et al., 2019).

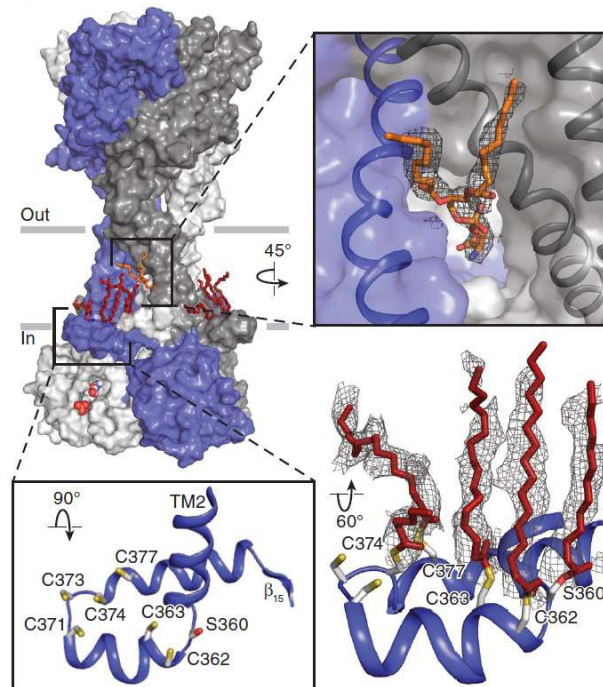


Figure 1.10: Depiction of C-cys anchor in rP2X7 receptor structure and in detail (bottom). Depiction of lipid moiety bound to transmembrane domain in rP2X7 receptor structure and in detail (upper right) (taken and adjusted from (McCarthy et al., 2019)).

#### 1.4.2. Lipid moiety bound between TM1 and TM2 domains:

P2X7 receptor activation was found to be linked to phosphatidylserine exposure and its presence in the outer membrane layer of the cell. It has been argued and theorized that the P2X7 receptor itself might be the cause of this phenomena, adding yet another function to this receptor (Sluyter, Shemon, & Wiley, 2007). Authors of the study that revealed the whole P2X7 receptor structure also found a lipid-like molecule bound at a site located between the receptor's transmembrane domains and C-cys anchor and they argue that the molecule may be phosphatidylserine and site might be a possible binding site for phosphatidylserine and thus serve in the flippase function of the P2X7 receptor (Fig. 1.10) (McCarthy et al., 2019).

#### 1.4.3. Cytoplasmic ballast:

Cytoplasmic ballast is a large structure located on the inner side of the cytoplasmic membrane. Its general shape resembles a globule. This feature consists of the aforementioned P2X7 receptor's large C-terminus and contains 200 amino acids. It is made of three

antiparallel  $\beta$  sheet and eight differently sized  $\alpha$  helices connected by loops (Fig. 1.11). The cryo-EM structure model of the P2X7 receptor however lacks a necessary resolution at a space of Ser443 and Arg471. This leads to uncertainty about the strands of subunits of which the cytoplasmic ballast is composed of. The authors of the study chose the simplest solution for this problem and assume, that each ballast is made of only single strand, however it might be possible, that it may be composed of two strands from two subunits (McCarthy et al., 2019).

The cytoplasmic ballast itself contains two features of interest, these being a  $Zn^{2+}$  binding site and bound GDP (Guanosine-5'-diphosphate), that was found to be bound in the cytoplasmic ballast (Fig. 1.11) (McCarthy et al., 2019).

There are two binding sites for  $Zn^{2+}$  in each P2X7 subunit. These binding sites are composed of seven cysteine residues, that form a tetrahedral structure within the cytoplasmic ballast. This feature seems to be important for receptor trafficking, as mutations of these cysteine residues cause the receptor not to be transported out of the endoplasmic reticulum and to be later degraded (Gonnord et al., 2009; McCarthy et al., 2019).

A GDP binding site with a GDP molecule bound was found in the cytoplasmic ballast of the P2X7 receptor (Fig.1.11). This site is located in between two cytoplasmic ballasts of two subunits. This site also has high affinity for GTP (Guanosine-5'-triphosphate) and GTP –  $\gamma$  – S and GDP molecule was found to be bound in open state as well as in closed state of the P2X7 receptor (McCarthy et al., 2019).

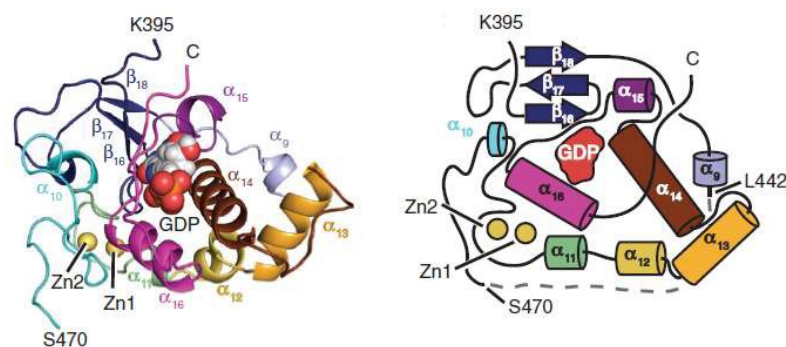


Figure 1.11: Structural (left) and an schematic (right) depiction of rP2X7 receptor cytoplasmic ballast structure (taken and adjusted from (McCarthy et al., 2019)).

#### 1.4.4. Signaling motifs in P2X7 receptor:

P2X7 receptor 's long C-terminus harbors many motifs and sequences, that are or could be considered as important for signaling or other functions besides channel function. However,

direct function or possible interaction of many of these is unknown, as these features could often be found inside of the cytoplasmic ballast and therefore inaccessible for solvent and molecules within it (Kopp et al., 2019; McCarthy et al., 2019).

Chain sequence-wise first feature, that can be found in what is considered C-tail of P2X7 receptor is the above-mentioned C-cys anchor with cysteine residues important for receptor trafficking and channel function (Gonnord et al., 2009; McCarthy et al., 2019). However, upstream and downstream of this feature, two other motifs have been found. These being the cholesterol recognition amino acid consensus motifs with a sequence of [(L/V)X1–5YX1–5(K/R)] (Robinson et al., 2014). Within the further of these motifs, three tyrosine residues are located, which can be phosphorylated by cellular sarcoma tyrosine kinase (Leduc-Pessah et al., 2017). Two possible actin binding sites were found nearby, located at 389 to 405 (in human P2X7 sequence) and 419 to 425 (in rat P2X7 sequence) (Denlinger et al., 2001; Gu et al., 2009; Kim et al., 2001; Watters et al., 2001).

Further on the C-terminal tail sequence, another potential motif is located. In the area of 438 to 533, a sequence similar to a death domain was discovered (Denlinger et al., 2001). Its identity to tumor necrosis factor receptor is up to 20% and its conservation is 50%. These domains are often associated with inflammation and apoptosis, similarly as P2X7 receptor itself. Within this area, a proline rich region is also present, containing two PxxP motifs, which could possibly bind cellular sarcoma tyrosine kinase homology 3 domain (Watters et al., 2001). Here and further along the P2X7 chain, in areas of 457 to 462 and 565 to 569, a sequence resembling dileucine motif ([D/E]xxxL[I/L]) has been found. This motif is associated with trafficking and sorting (Kozik, et al, 2010; Wiley et al., 2011).

There are also several other cysteine residues, that are known to be palmitoylated across a wide section of the P2X7 receptor's C-tail. These are located on positions of 477, 479, 482, 498, 499, 506, 572 and 573 in the sequence of the C-terminus and they are considered to be important for receptor trafficking import into membrane, as mutations of these cysteine residues led to lower expression on the membrane (Gonnord et al., 2009).

In the 541 to 560 area of the chain, a ([I-x(3)-L-x(10)-W]) sequence was discovered. This sequence represents a calmodulin binding motif. P2X7 receptor is permeable to calcium ions, thus being important for calmodulin, a calcium sensing protein (Roger, Pelegrin, & Surprenant, 2008).

It is theorized that in the area of 551 to 581 of the sequence, a retention motif is located. Truncations and mutations of this area and its surrounding have been reported to cause loss of surface membrane expression, and it has been suggested that these changes lead

to exposure of the motif, thus keeping the subunits from being present on the membrane (Smart et al., 2003).

A lipid interaction or lipopolysaccharide (LPS)-binding motif was found located on 574 to 589 sequence. It is homologous to LPS binding domains of other proteins and is known to bind LPS in *in vitro* conditions. It has also been suggested that this motif may bind membrane phospholipids as well, therefore possibly modulating the receptor localization within the membrane itself, such as localizing the P2X7 receptor into lipid rafts (Denlinger et al., 2001).

#### 1.4.5. P2X7 and phagocytosis:

P2X7 receptor has been shown to mediate phagocytosis in transfected HEK 293 cells and to function as a scavenger receptor in the brain (Gu et al., 2011). Macrophages, natively expressing relatively lot of P2X7, and P2X7 transfected HEK 293 cells were observed to phagocyte neuronal cells and lymphocytes in media free of serum. It was observed, that the P2X7 receptor expressing cell require absence of serum and it can thus be theorized, that the P2X7 mediated phagocytosis only takes place in central nervous system, where cerebrospinal fluid is present. HEK 293 cells transfected with P2X7 are also known to phagocyte latex beads (Gu et al., 2009; Gu et al., 2010; Gu & Wiley, 2018).

It was also shown that activation of P2X7 receptor leads to decrease of phagocytotic activity and has been linked with P2X7 receptor's disassociation from complex with non-muscle myosin, that could be, at least partially, responsible for the phagocytic activity (Gu et al., 2009). Inhibition of the ion channel activity of P2X7 receptor generally did not affect its phagocytic effect, with the only exception being oxidized ATP, which inhibits both the channel activity and the phagocytic activity. Inhibition of P2X7 receptor by its specific inhibitor also inhibited the decrease in phagocytosis of microglial cells stimulated by BzATP (Ou, Gu, & Wiley, 2018; Tao et al., 2022). Mitochondrial dynamics are thought to be at least partly responsible for this phenomenon (Tao et al., 2022).

Three parts of the receptor chain have been suggested to be responsible for the binding of the receptor to the phagocytosed object. These are composed of residues numbered 115 to 128, 129 to 143 and 150 to 162 that were shown to selectively bind to apoptotic cell. Each of these sequences contains a cysteine residue, mutation of which leads to loss of its binding function. It has also been observed, that after treatment with thiol compounds, the phagocytotic activity was inhibited, thus leading to a conclusion that thiol and/or disulfide

bridges play a role in P2X7 receptor's interaction and binding to phagocytosed material (Gu et al., 2011).

#### 1.4.6. P2X7 receptor's role in metabolism and mitochondria:

P2X7 receptor was originally supposed to regulate cellular metabolism (Adinolfi et al., 2005). However, the authors of more recent a study claimed, they detected P2X7 receptor on the mitochondrial membrane. According to them, it is supposed to be present on the outer membrane, with the large extracellular loop facing cytosolic space and N- and C- termini facing the intermembrane space. It was observed that cells with induced P2X7 receptor expression have higher calcium levels in their mitochondria matrix and cells that normally express P2X7 have their matrix calcium level diminished when P2X7 receptor expression is knocked-down (Sarti et al., 2021).

Respiratory chain complex I activity was increased in cells expressing P2X7 receptor, which led to the above-mentioned increase in calcium levels. It is however yet unknown, how P2X7 affects NADH dehydrogenase (Sarti et al., 2021). P2X7 receptor has also been observed to affect the shape and volume of mitochondria, as a recent study also observed (Tao et al., 2022).

Mitochondria of microglial cell were observed to branch significantly more after being treated with BzATP. This led the authors to the conclusion, that P2X7 receptor activation may also lead to mitochondrial fission. This, the authors argue, is caused by P2X7-induced calcium influx, that increases the activity of calcineurin, which in turn leads to dephosphorylation of Ser637 of dynamin-related protein 1. According to the study, it is excessive mitochondrial fission, that causes the impairment of phagocytosis after P2X7 receptor activation (Tao et al., 2022).

#### 1.4.7. P2X7 receptor's role in phosphatidylserine exposure:

Various studies have shown, that P2X7 receptor activation is linked with phosphatidylserine exposure on the outer cell membrane surface (Sluyter et al., 2007). It is well established that this molecule plays an important role in signaling, particularly in immune system and in cell death, as apoptotic cells expose this molecule (Schlegel & Williamson, 2001). One study determined that calcium is not a primary or sole cause of phosphatidylserine exposure in ATP stimulated cells and that sodium however has significant effect on the P2X7-induced exposure (Courageot et al., 2004).

As was mentioned in previous chapter, a lipid moiety has been found in cryo-EM structure of the P2X7 receptor, bound between the two transmembrane domains. Even though the identity of this molecule is unsure, the authors claim that this moiety might possibly be phosphatidylserine (McCarthy et al., 2019).

A recent study found that P2X7-induced phosphatidylserine exposure is dependent on presence of two other proteins, these being Xk and Vps13a. The same study also identified EROS as important for P2X7 function, as it seems to act as a chaperone to P2X7 receptor and assist in its folding (Ryoden, Segawa, & Nagata, 2022). Xk is member of Xkr family of scramblases and Vps13a belongs to VPS13 family, that are known to form conduits between membranes of various organelles, thus allowing for lipid transport. These two proteins were shown to interact. It is however yet unknown by what mechanism would these proteins play a role in phosphatidylserine exposure induced by P2X7 activation (Leonzino, Reinisch, & De Camilli, 2021; Ryoden et al., 2022; Sassenbach, 2022; Suzukit et al., 2013).

#### 1.4.8. P2X7 in sperm:

It has been revealed that purinergic receptors, including several P2X receptors (P2X7 among them), are present in testicular tissues and cell types (Fleck et al., 2016; Glass et al., 2001; Mundt, Kenzler, & Spehr, 2022). However, it has been relatively recently discovered, that ATP presence in capacitating media can induce acrosomal reaction in rat sperm, though purinergic signaling being involved in acrosomal reaction is not new (Luria, Rubinstein, Lax, & Breitbart, 2002; Torres-Fuentes, Rios, & Moreno, 2015).

This phenomenon was further examined by adding different inhibitors of P2 receptors. P2X receptor inhibitors were observed to also inhibit ATP induced acrosomal reaction, in particular P2X7 specific antagonists led to the inhibition and BzATP, a highly potent P2X7 agonist, caused acrosomal reaction in several fold lower concentration than ATP itself. Immunostaining then revealed, that P2X7 can be found principal piece and the acrosomal region of the head of the sperm (Torres-Fuentes et al., 2015). Authors claim that there is high enough concentration of extracellular ATP within oviduct during the oestrous stage to possibly trigger ATP-induced P2X- mediated acrosomal reaction. This phenomenon however seems to function differently among different species (Torres-Fuentes et al., 2015).

#### 1.4.9. Receptor sensitization and deactivation:

P2X7 receptor activation shows so called “run up”, it means a rise in current amplitude upon prolonged or repeated agonist application. This yet unexplained feature of P2X7 was originally thought to be connected with its ability to accumulate large organic cations and fluorescent dyes and was referred to as pore dilatation. Thus, P2X7 was thought to be capable of time-dependent changes in its conductivity state, somehow widening the ion passage pathway, and forming some sort of macropore, that is more readily permeable to larger molecules (North, 2002; Surprenant et al., 1996; C. Virginio et al., 1999). This behavior of P2X7 was thought to be due to its inherent characteristic, with P2X7 receptor's long C-terminus having an important role in macropore formation and dynamics (Di Virgilio et al., 2018; Feng et al., 2006).

However, it was later revealed, through single channel patch clamp recording, that P2X7 channel does not change its state into any sort of macropore during prolonged agonist stimulation. These measurements showed that the amplitude of single channel-mediated currents remained unchanged throughout the whole recording and that large organic molecules can pass through the pore immediately after receptor activation (Riedel, Schmalzing, & Markwardt, 2007). Another study showed that P2X7 increases its open state duration after sensitization with two conductive states,  $O_1$  and  $O_2$ , being present both in naïve and sensitized states.  $O_2$  is of higher conductance than  $O_1$  (Dunning et al., 2021).

Deactivation of the receptor can be measured as a decay of current after unbinding of an agonist. In channels that do not desensitize, reflects the channel conformation change from open to closed state (Colquhoun, 1998). It is theorized, that it is the agonist unbinding, that is the rate limiting step of the deactivation (Zemkova et al., 2004). Rates of current decay were measured in several P2X receptors and were mostly observed to be well defined by mono-exponential functions in whole-cell patch clamp recording, such as in cells expressing both P2X2<sub>A</sub> and P2X2<sub>B</sub> and in most of the cells expressing some variants of chimeric P2X2<sub>A</sub>/3 receptors. P2X1/3 chimeras were also observed to deactivate monoexponentially. Deactivation kinetics is also dependent of concentration of agonist (Rettinger & Schmalzing, 2004; Zemkova et al., 2004). P2X7 deactivation was observed to follow both mono-exponential and biexponential function, with differences induced by mutations in the N-terminal, and that deactivation is elongated upon repeated agonist application (Yan et al., 2010). The mechanisms underlying this prolongation are still unknown.

## **2. Aims of the study**

The aim of this diploma thesis was to understand the role of the first transmembrane domain (TM1) in P2X7 deactivation and dye uptake function, and identify TM1 residues that play a key role in these processes. Particular tasks were as follows:

1. To culture and transfect human embryonic kidney 293T cells (HEK-293T) with rat P2X7 wildtype receptor (P2X7-WT) or single point TM1 mutants that were previously generated in our laboratory.
2. Using electrophysiological patch clamp technique to study the decay of current stimulated by activation of naïve P2X7 receptors and receptors sensitized by prolonged stimulation with agonist.
3. To evaluate deactivation kinetics of P2X7-WT and mutated receptors by biexponential fitting of decay of current after agonist washout.
4. Using microfluorimetric measurements to study EtBr uptake by HEK-293T cells expressing selected TM1 mutants.
5. To discuss the role of individual TM1 residues that control P2X7 deactivation and dye uptake function using molecular model of rat P2X7.

### 3. Material and methods

#### 3.1. Chemicals:

BzATP	Sigma, USA
Trypsin	GIBCO, USA
DMEM	GIBCO, USA
Bovine serum	GIBCO, USA
Versene	GIBCO, USA
Streptomycin	GIBCO, USA
Penicillin	GIBCO, USA
Ethidium bromide	Sigma, USA
NaCl	Sigma, USA
KCl	Sigma, USA
MgCl <sub>2</sub>	Sigma, USA
CaCl <sub>2</sub>	Sigma, USA
HEPES	Sigma, USA
D-Glucose	Sigma, USA
NaOH	Sigma, USA
EGTA	Sigma, USA
CsCl	Sigma, USA
CsOH	Sigma, USA
EGTA	Sigma, USA

#### 3.2. DNA constructs:

Rat full-length P2X7 (rP2X7) cDNA subcloned into the bicistronic enhanced fluorescent protein expression vector, pIRES2-EGFP (Clontech, Mountain View, CA, USA) was a gift from Dr S.S. Stojilkovic, NICHD/NIH, Bethesda, USA. Alanine substitutions of TM1-P2X7 used in this diploma thesis were recently generated in laboratory to study the role of TM1 in P2X7 function (Rupert et al., J.Neurochem, submitted). Substitution with alanine is generally used to determine the influence of polarity, charge or other properties of original amino acid on receptor structure and function.

### **3.3. Cell culturing and transfection:**

Human embryonic kidney 293T cells (HEK293T; American Type Culture Collection, Rockville, MD, USA) were cultured for the experiments. These cells were cultured and grown in 75 cm<sup>2</sup> plastic culture flasks (NUNC, Rochester, NY), in a humidified 5% CO<sub>2</sub> atmosphere at 37°C, in Dulbecco's modified Eagle's medium that has been supplemented by addition of 10% fetal bovine serum, 50 U/ml penicillin and 50 µg/ml streptomycin. The cells were grown in these conditions for 48 - 72 hours, until 80-90% confluence was reached. Then the cells were passaged.

During the passaging, the cells were washed by 10 ml Versene and then detached by digestion with 1 ml trypsin (0,5%). Trypsin digestion was stopped by addition of sufficient volume of growth medium. Cells were then centrifuged for 5-10 min at 900 g, the formed pellet washed by growth medium and resuspended in growth medium. Part of the suspension was then added into new 75 cm<sup>2</sup> plastic culture flasks for further culturing.

Day before transfection, approximately 150000 cells were seeded directly onto 35mm culture dishes (Sarstedt, Newton, NC) with 2 ml of the above-mentioned medium, if these cells were later used for electrophysiological measurements. Alternatively, the cells were seeded onto 12mm coverslips (Glaswarenfabrik Karl Hecht KG, Sandheim, Germany), coated with poly-L-lysine, that were put into the aforementioned dishes (3 coverslips per dish), if the cells were used for microfluorometric experiments.

Transfection was performed using 2 µg of DNA and 2 µl of jetPRIME<sup>TM</sup> reagent in 2 ml of Dulbecco's modified Eagle's medium according to the manufacturer's instructions (PolyPlus-transfection, Illkirch, France). For use in electrophysiological experiments, the transfected cells were mechanically dispersed after 24 h of incubation, cells were re-seeded on 35 mm Corning 3294 CellBIND Surface dishes (Corning, NY, USA) for 2 - 4 hours prior to recording. For the dye uptake measurements, the transfected cells plated on 12 mm poly-L-lysine-coated coverslips were not dispersed prior to measurements.

### **3.4. Patch clamp recordings:**

Patch clamp whole-cell recording was performed using Axopatch 200B patch-clamp amplifier (Axon Instruments, Union City, CA). The recorded data were captured and stored by pClamp 9.0 software package with Digidata 1322A A/D converter (Axon Instruments). During recording, the cells were continuously perfused at a flow rate of 2 ml/minute, with an extracellular solution containing: 142 mM NaCl, 2 mM CaCl<sub>2</sub>, 3 mM KCl, 1 mM MgCl<sub>2</sub>, 10

mM HEPES and 10 mM D-glucose. The pH of this medium was adjusted to 7,3 by addition of needed amount of NaOH. The osmotic pressure of the medium was 293 mOsm. The intracellular solution, that was used to fill the patch electrodes, contained: 11 mM EGTA, 10 mM HEPES, 154 mM CsCl. The pH of the intracellular solution was adjusted to 7,2 by addition of CsOH. The osmotic pressure of the medium was 300mOsm.

All solutions with agonists were prepared in the day of experiment and were applied using the RSC-200 Rapid Solution Changer (Biologic, Claix, France). The measurements were performed on single cells with average capacitance being about 10 pF and the membrane potential was held at -60mV.

Glass electrodes were pulled using a Flaming Brown horizontal electrode puller (Model P-97; Sutter Instruments, Novato, CA) and polished by using a heat polisher (Model MF-830; Narishige, Tokyo, Japan) to a final electrode resistance of 5-8 M $\Omega$ . As recording electrode Ag/AgCl wire was used, the reference electrode was Ag/AgCl pellet. The transfection efficiency was identified by monitoring the fluorescence of EGFP under UV light using the Olympus IX71 inverted fluorescent microscope.

The protocol used for obtaining patch clamp results was as follows: After the whole cell patch was established, solution of 100  $\mu$ M BzATP was applied to the recorded cell for 2 – 5 s. Afterwards, the BzATP was washed out by 30 s long application of extracellular solution. Solution of 100  $\mu$ M BzATP was then applied for 60 s, and then washed out by 30 s long application of extracellular solution. Finally, 100  $\mu$ M BzATP was applied again for 2 – 5 s.

### **3.5. Ethidium bromide uptake:**

Accumulation of ethidium bromide was measured on cells cultured on glass coverslips. The imaging was done using 40x water immersion objective at room temperature (20–25°C) on epifluorescent microscope (Olympus BX50WI, Melville, NY, USA). The changes in fluorescence were recorded by MicroMAX CCD camera (Princeton Instruments; Roper Scientific GmbH, Martinsried, Germany). The software used to control the hardware and later analysis was MetaFluor software (Molecular Devices, Downingtown, PA). Ethidium bromide was excited at 526nm and emission was recorded at 605nm. The average fluorescence signal of 5-10 cells on each coverslip was calculated. During experiment, the cells were perfused with extracellular solution using the RSC-200 Rapid Solution Changer (Biologic, Claix, France).

Each mutation's and P2X7-WT receptor was measured according to two protocols. According to the first protocol, solution of 20 $\mu$ M ethidium bromide was applied for 30s. Then solution of 100  $\mu$ M BzATP and 20 $\mu$ M ethidium bromide was applied for 60s, after which solution of 20 $\mu$ M ethidium bromide was applied for another 30s. According to the second protocol, solution of 100 $\mu$ M BzATP was applied for 60s. The BzATP solution was then washed out by applying extracellular solution for 60s. Afterwards, solution of 20 $\mu$ M ethidium bromide was applied for 30s. Then solution of 100 $\mu$ M BzATP and 20 $\mu$ M ethidium bromide was applied for 60s, after which solution of 20 $\mu$ M ethidium bromide was applied for another 30s.

### **3.6. Calculations:**

The electrophysiological recordings were evaluated by pClamp. The current decay evoked by agonist washout was fitted with doubleexponential function ( $y = A_{\text{slow}} \exp(-t/\tau_{\text{slow}}) + A_{\text{fast}} \exp(-t/\tau_{\text{fast}})$ ) function, where  $A_{\text{slow}}$  and  $A_{\text{fast}}$  are amplitudes of the decay affected by each exponential and  $\tau_{\text{slow}}$  and  $\tau_{\text{fast}}$  are time constants defining each exponential. Weighted average of these time constants ( $\tau_{\text{weight}}$ ) was calculated as  $y = [(A_{\text{slow}} * \tau_{\text{slow}}) + (A_{\text{fast}} * \tau_{\text{fast}})] / (A_{\text{slow}} + A_{\text{fast}})$ .

All numerical values in the text are reported as the mean  $\pm$  SEM. Significant differences (\*\*p < 0,01 and \*p < 0,05) between means were evaluated by unpaired t-test using SigmaStat 2000 v9.01.

## 4. Results

### 4.1. Electrophysiological patch clamp recordings:

P2X7-WT and alanine substitutions of its TM1 domain (TM1 mutants) were expressed in HEK293 cells and examined using electrophysiological patch clamp method. After whole-cell patch clamp recording was established, the cells were stimulated by 100  $\mu$ M solution of BzATP for 2-5 s to produce short naïve response (naïve means that agonist was not yet applied and cell was not yet stimulated). Approximately 30s after naïve response, 100  $\mu$ M solution of BzATP was applied again for 60 s. This led to biphasic response with secondary growing current and sensitization of the receptor. After 30s of agonist washout, 100  $\mu$ M BzATP was applied again for 2-5 s to produce short sensitized response (Fig. 4.1).

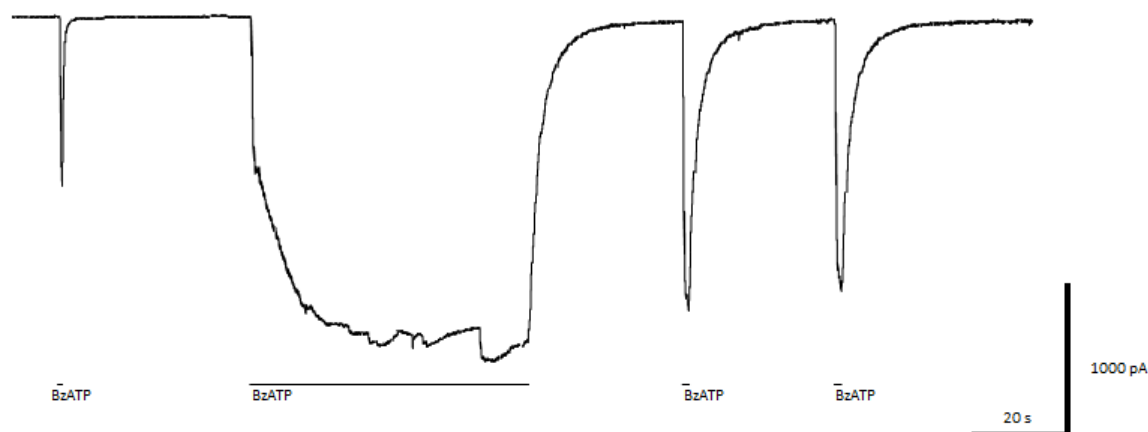


Figure 4.1: Example of whole-cell patch clamp recording of P2X7-WT current stimulate by application of BzATP according to the described protocol. The lines under the recording labeled “BzATP” indicate duration and time when 100  $\mu$ M BzATP was applied.

Current decay after washout of agonist was evaluated by fitting. The biexponential function was found to be the best fit to describe deactivation kinetics of both naïve and sensitized responses, of both P2X7-WT and TM1 mutants. This biexponential is composed of two components: fast component and slow component. Four parameters were evaluated for each response based on fitting with biexponential function:  $\tau_{\text{fast}}$  and  $\tau_{\text{slow}}$  (which are deactivation time constants describing their respective components), contribution of  $\tau_{\text{fast}}$  to the whole current decay (in %) and  $\tau_{\text{weight}}$  (weight arithmetic mean of  $\tau_{\text{fast}}$  and  $\tau_{\text{slow}}$ ) (Fig. 4.2).

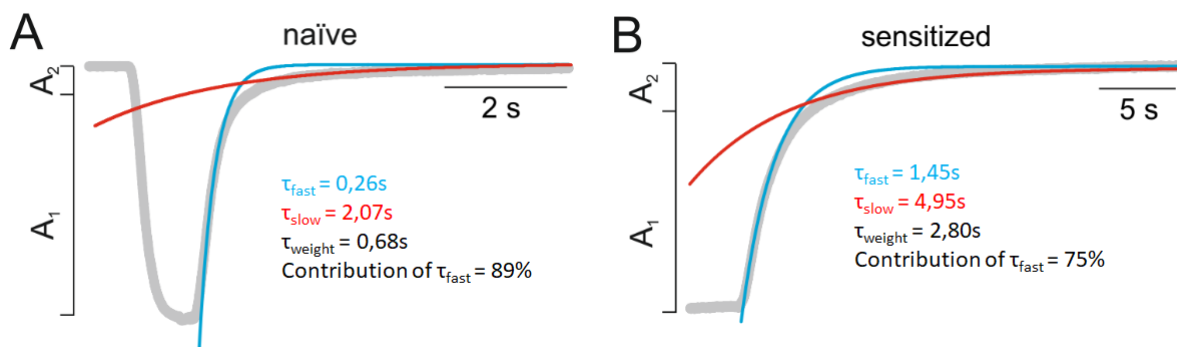


Figure 4.2: Example of biexponential fitting of current decay of responses to 100  $\mu\text{M}$  BzATP in naïve (A) and sensitized (B) P2X7-WT. The values below traces are results of this particular biexponential fitting.  $A_1$  and  $A_2$  are the relative amplitudes of the fast ( $\tau_{\text{fast}}$ , blue lines) and slow ( $\tau_{\text{slow}}$ , red lines) deactivation time constants, respectively, which were used to calculate the weight deactivation time constant ( $\tau_{\text{weight}}$ ). The contribution of  $\tau_{\text{fast}}$  was calculated as the  $A_1$  to  $(A_1+A_2)$  ratio (in %) (Rupert et al., submitted).

#### 4.1.1. Deactivation kinetics of naïve P2X7-WT and TM1 mutants:

Naïve responses of P2X7-WT exhibited following deactivation parameters:  $\tau_{\text{weight}} = 0,51 \pm 0,07$  s;  $\tau_{\text{fast}} = 0,24 \pm 0,02$  s;  $\tau_{\text{slow}} = 3,17 \pm 0,7$  s; contribution of  $\tau_{\text{fast}} = 89,6 \pm 0,1\%$  ( $n=22$  cells). This indicates that fast component is responsible for almost 90% of the current decay, and the slow component, which is about 13 times longer, affects only about 10% of the current decay in P2X7-WT naïve receptor.

Next, the deactivation kinetics of naïve responses were examined in TM1 mutants. Seven of 21 TM1 mutations could not be measured, since the current amplitude stimulated by application of 100 $\mu\text{M}$  solution of BzATP was not high enough to allow for biexponential fitting. The amplitude of responses in these mutations reached only tens of pA, and the BzATP-stimulated currents were unrecognizable from electrical noise. These so-called “non-functional” mutations are: Lys30Ala, His34Ala, Tyr40Ala, Phe43Ala, Leu45Ala, Met46Ala and Asp48Ala. Remaining mutations showed current amplitude comparable with that of P2X7-WT receptor, except Gly27Ala and Val41A that exhibited current amplitude significantly lower compared to P2X7-WT (Table 1).

Several TM1 mutations differed in their  $\tau_{\text{weight}}$  of naïve response from that of naïve P2X7-WT with high statistical significance ( $P < 0,01$ ) These mutations are: Gly27Ala ( $\tau_{\text{weight}} = 1,96 \pm 0,34$  s), Trp31Ala ( $\tau_{\text{weight}} = 1,53 \pm 0,48$  s), Leu33Ala ( $\tau_{\text{weight}} = 3,23 \pm 10,1$  s), Thr36Ala ( $\tau_{\text{weight}} = 0,92 \pm 0,14$  s), Val41Ala ( $\tau_{\text{weight}} = 4,02 \pm 0,89$  s). Mutations Ser39Ala ( $\tau_{\text{weight}} = 0,97$

$\pm 0,35$  s) and Ser42Ala ( $\tau_{\text{weight}} = 0,83 \pm 0,1$  s) differed as well, but with less statistical significance ( $P < 0,05$ ) (Fig. 4.3).

Table 1: Characterization of single point TM1 mutants of rat P2X7

	$\tau_{\text{weighed}}$ (s)	SE	$\tau_{\text{slow}}$ (s)	SE	$\tau_{\text{fast}}$ (s)	SE	Contribution of $\tau_{\text{fast}}$ (%)	SE	I (nA)	SE	EC50	SE
rP2X7WT	0,51	0,07	3,17	0,70	0,24	0,02	89,63	0,98	1,2	0,1	43	3
	1,26	0,21	4,33	0,60	0,54	0,05	79,44	2,21	1,7	0,1	31	2
G27A	1,96**	0,34	4,43*	0,26	0,22*	0,03	58,06**	10,95	0,24	0	49	3
	2,64**	1,33	8,37*	3,40	0,25*	0,05	79,36	4,94	0,61	0	46	4
T28A	0,77	0,24	2,62	0,79	0,30	0,07	81,16**	3,15	1,2	0,1	63	5
	1,13	0,39	3,33	1,05	0,64	0,18	80,38	4,62	1,6	0,2	49	5
I29A	0,36	0,04	2,68	0,55	0,17	0,01	91,34	2,29	1	0,1	66	9
	1,11	0,30	3,78	0,80	0,57	0,07	81,94	2,67	1,3	0,1	43	7
K30A	0,00	0,00	0,00	0,00	0,00	0,00	0,00	0,00	0,25	0	>100	
	0,00	0,00	0,00	0,00	0,00	0,00	0,00	0,00	0,43	0,1	>100	
W31A	1,53**	0,48	5,71	1,43	0,22	0,05	77,44**	3,01	1,1	0,1	39	4
	2,01	0,84	9,17	1,77	0,45**	0,10	84,84	2,81	1,5	0,1	33	3
I32A	0,34	0,07	1,78	0,19	0,20	0,03	90,33	2,76	1,6	0,3	42	7
	2,02	1,11	5,11	1,95	0,60	0,18	65,80	6,35	1,8	0,3	27	5
L33A	3,23**	1,01	6,96*	1,73	0,48**	0,13	63,22**	6,45	1	0,1	30	6
	4,35**	1,93	9,91	2,12	0,57	0,07	65,58	5,96	1,4	0,2	25	3
H34A	0,00	0,00	0,00	0,00	0,00	0,00	0,00	0,00	0,25	0,1	>100	
	0,00	0,00	0,00	0,00	0,00	0,00	0,00	0,00	0,3	0,1	>100	
M35A	0,60	0,09	2,88	0,56	0,27	0,01	87,80	1,40	1,1	0,2	39	5
	1,54	0,23	4,15	0,69	0,75	0,10	74,39	5,22	1,6	0,1	22	4
T36A	0,92**	0,14	5,77	1,26	0,33	0,02	88,59	1,79	1,1	0,2	46	6
	1,81	0,95	3,60	1,14	0,72	0,16	76,97	6,70	1,6	0,2	19	2
V37A	0,56	0,08	2,01	0,18	0,33	0,03	85,88	2,75	1,4	0,1	43	7
	1,93	0,99	4,48	1,51	0,66	0,17	71,78	5,52	1,5	0,1	22	4
F38A	1,01	0,40	4,63	2,31	0,39**	0,06	86,54	2,52	1,3	0,2	39	7
	3,73**	2,03	9,66*	4,72	0,78*	0,08	67,59	9,74	1,5	0,2	25	3
S39A	0,97*	0,35	5,67	2,03	0,28	0,02	88,36	2,16	1,5	0,2	49	6
	2,55*	0,99	6,22	2,80	0,53	0,17	64,92*	6,35	1,9	0,2	26	4
Y40A	0,00	0,00	0,00	0,00	0,00	0,00	0,00	0,00	0,37	0,1		
	0,00	0,00	0,00	0,00	0,00	0,00	0,00	0,00	0,22	0,1		
V41A	4,02**	0,89	13,7**	3,91	0,92**	0,17	73,34**	4,72	0,6	0,1	44	5
	11,86**	5,25	29,1**	11,4	1,10**	0,08	64,39**	4,19	1,1	0,3	28	4
S42A	0,83*	0,10	4,86	1,27	0,28	0,03	83,86*	2,32	1,4	0,2	38	5
	1,46	0,23	3,93	0,92	0,72	0,18	77,10	1,28	1,7	0,2	22	2
F43A	0,00	0,00	0,00	0,00	0,00	0,00	0,00	0,00	0,08	0		
	0,00	0,00	0,00	0,00	0,00	0,00	0,00	0,00	0,09	0		

A44L	0,40 1,52	0,04 0,66	1,54 7,75	0,38 2,60	0,23 0,40	0,02 0,04	84,67 85,54	3,98 1,36	1,3 1,5	0,2 0,2	38 36	4 4
L45A	0,00 0,00	0,00 0,00	0,00 0,00	0,00 0,00	0,00 0,00	0,00 0,00	0,00 0,00	0,00 0,00	0,25 0,25	0,1 0,1		
M46A	0,00 0,00	0,00 0,00	0,00 0,00	0,00 0,00	0,00 0,00	0,00 0,00	0,00 0,00	0,00 0,00	0,18 0,14	0 0		
S47A	0,53 2,78*	0,09 1,49	2,14 9,28*	0,27 4,18	0,25 0,57	0,02 0,16	85,84 76,94	2,71 6,15	1,2 1,6	0,1 0,2	44 31	6 4
D48A	0,00 0,00	0,00 0,00	0,00 0,00	0,00 0,00	0,00 0,00	0,00 0,00	0,00 0,00	0,00 0,00	0,34 0,38	0 0,1	>100 >100	

Table 1. contains and of  $\tau_{\text{weight}}$ ,  $\tau_{\text{slow}}$ ,  $\tau_{\text{fast}}$  and contribution of  $\tau_{\text{fast}}$  values and their respective standard error of P2X7-WT and each mutation. Values of naïve responses are in black, values of sensitized responses are in blue. The table also contains maximum peak current (I) and EC<sub>50</sub> values (the agonist concentration producing 50% of the maximal response, in  $\mu\text{M}$ ) for P2X7-WT each mutation and which are taken from submitted manuscript ((Rupert et al., submitted). (\*\*) indicates statistically highly significant ( $P < 0,01$ ) difference between P2X7-WT and mutant and (\*) indicates statistically significant ( $P < 0,05$ ) difference between P2X7-WT and mutant. Data were derived from 3 to 12 measurements per mutant.

It is conceivable that the observed changes in  $\tau_{\text{weight}}$  were accompanied by changes in  $\tau_{\text{fast}}$ , or contribution of  $\tau_{\text{fast}}$  or  $\tau_{\text{slow}}$  or by changes in all these parameters.

As far as the  $\tau_{\text{slow}}$  parameter is concerned, the only mutation that differed with high statistical significance ( $P < 0,01$ ) from the P2X7-WT was Val41Ala ( $\tau_{\text{slow}} = 13,7 \pm 3,91$  s). Two other mutations differed in  $\tau_{\text{slow}}$  as well, but less significantly ( $P < 0,05$ ). These are Gly27Ala ( $\tau_{\text{slow}} = 4,43 \pm 0,26$  s) and Leu33Ala ( $\tau_{\text{slow}} = 6,96 \pm 1,73$  s) (Fig. 4.4).

The mutations, that differ with high statistical significance ( $P < 0,01$ ) from the P2X7-WT in  $\tau_{\text{fast}}$  are Leu33Ala ( $\tau_{\text{fast}} = 0,48 \pm 0,13$  s), Phe38Ala ( $\tau_{\text{fast}} = 0,39 \pm 0,06$  s) and Val41Ala ( $\tau_{\text{fast}} = 0,92 \pm 0,17$  s). Another mutation that differed in  $\tau_{\text{fast}}$  from P2X7-WT, but less significantly ( $P < 0,05$ ), is Gly27Ala ( $\tau_{\text{fast}} = 0,22 \text{ s} \pm 0,03$  s) (Fig. 4.4).

In the contribution of  $\tau_{\text{fast}}$ , five mutations differed with high statistical significance ( $P < 0,01$ ) from P2X7-WT receptor, these being Gly27Ala (contribution of  $\tau_{\text{fast}} = 58,0,6 \pm 10,95\%$ ), Thr28Ala (contribution of  $\tau_{\text{fast}} = 81,16 \pm 3,15\%$ ), Trp31Ala (contribution of  $\tau_{\text{fast}} = 77,44 \pm 3,01\%$ ), Leu33Ala (contribution of  $\tau_{\text{fast}} = 63,22 \pm 6,45\%$ ) and Val41Ala (contribution of  $\tau_{\text{fast}} = 73,34 \pm 4,72\%$ ). Mutation Ser42Ala (contribution of  $\tau_{\text{fast}} = 83,86 \pm 2,32\%$ ) also differed, but with lower statistical significance ( $P < 0,05$ ). (Fig. 4.4)

Number of cells that was used for this analysis is as follows: Gly27Ala (n= 6 cells), Thr28Ala (n= 6 cells), Trp31Ala (n= 7 cells), Leu33Ala (n= 6 cells), Thr36Ala (n= 8 cells), Phe38Ala (n= 10 cells), Ser39Ala (n= 7 cells), Val41Ala (n= 4 cells), Ser42Ala (n= 9 cells).

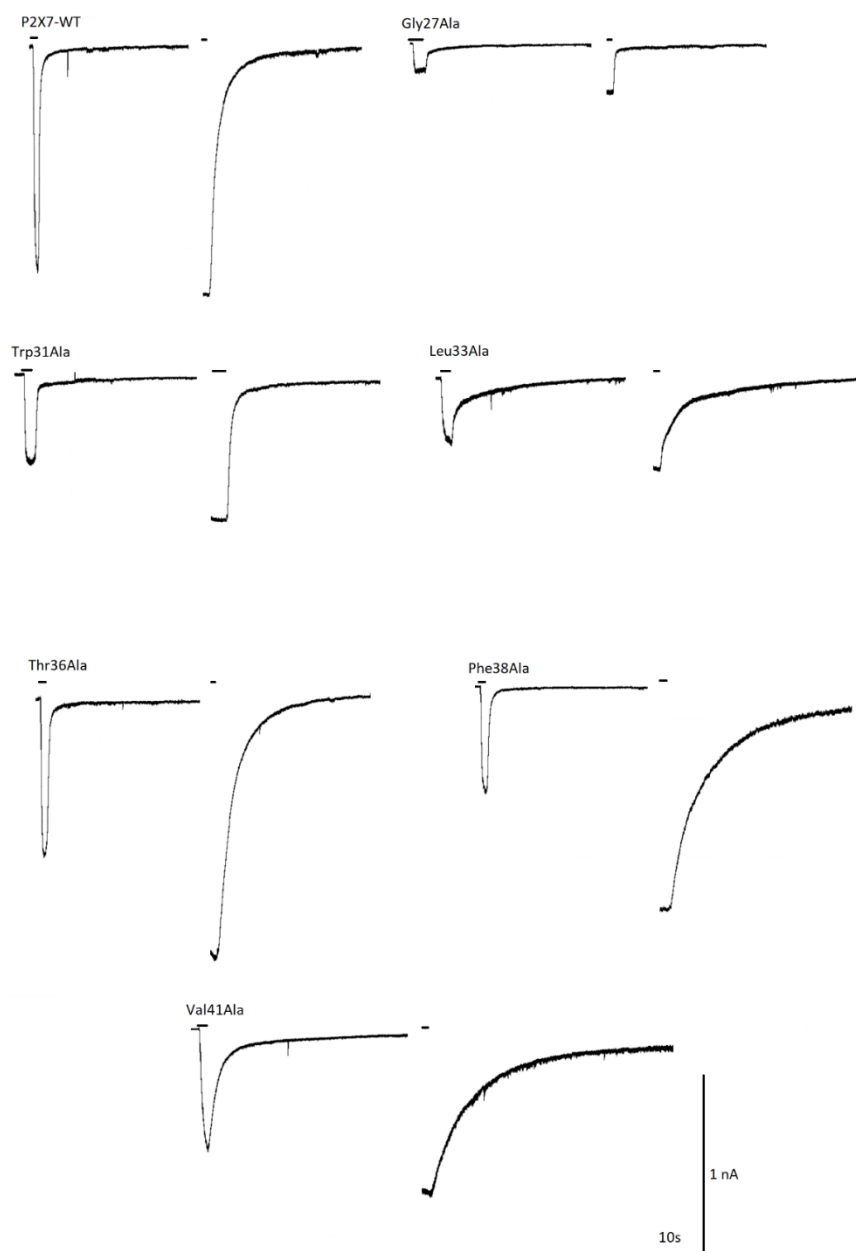


Figure 4.3. Example of naïve response (left) and current decay of sensitized response (right) of P2X7-WT and identified mutations that exhibited statistically highly significant changed  $\tau_{\text{weight}}$  compared to that of WT. The black lines above the recording mark the duration of BzATP application.



Figure 4.4: Effect of mutation of TM1-P2X7 residues on  $\tau_{\text{weighted}}$  (A),  $\tau_{\text{slow}}$  (B),  $\tau_{\text{fast}}$  (C) and contribution of  $\tau_{\text{fast}}$  (D) values in naïve responses to 100  $\mu\text{M}$  BzATP application. (\*\*) indicates statistically highly significant ( $P < 0,01$ ) difference between P2X7-WT and mutant and (\*) indicates statistically significant ( $P < 0,05$ ) difference between P2X7-WT and mutant as determined by unpaired t-test. ND = not determined.

#### 4.1.2. Deactivation kinetics of sensitized P2X7-WT and TM1 mutants:

After prolonged exposure of P2X7-WT to 100  $\mu$ M solution of BzATP, sensitized responses showed these values:  $\tau_{\text{weight}} = 1,26 \pm 0,21$  s,  $\tau_{\text{fast}} = 0,54 \pm 0,05$  s,  $\tau_{\text{slow}} = 4,33 \pm 0,6$  s and contribution of  $\tau_{\text{fast}} = 79,44 \pm 2,21\%$  on average (n=35 cells). All the sensitized values differ statistically highly significantly from their counterparts in naïve state of receptor, with the exception of  $\tau_{\text{slow}}$ , that was not statistically significant different from that of naïve P2X7-WT. These results indicate that current decay was prolonged in sensitized state about 2,5 fold due to increased  $\tau_{\text{fast}}$  value and also due to decreased  $\tau_{\text{fast}}$  contribution to deactivation kinetics.

Several mutations differed in their  $\tau_{\text{weight}}$  of sensitized response from P2X7-WT with high statistical significance (P<0,01). These are Gly27Ala ( $\tau_{\text{weight}} = 2,64 \pm 1,33$  s), Leu33Ala ( $\tau_{\text{weight}} = 4,35 \pm 1,93$  s), Phe38Ala ( $\tau_{\text{weight}} = 3,73 \pm 2,03$  s) and Val41Ala ( $\tau_{\text{weight}} = 11,86 \pm 5,25$ s). Two other mutations differed less significantly (P<0,05). These are Ser39Ala ( $\tau_{\text{weight}} = 2,55 \pm 0,99$  s) and Ser47Ala ( $\tau_{\text{weight}} = 2,78 \pm 1,49$  s) (Fig. 4.3 and 4.5).

Sensitization was also accompanied by significant changes in other parameters that were used to calculate  $\tau_{\text{weight}}$ . As far as the  $\tau_{\text{slow}}$  parameter is concern, two mutations differed with high statistical significance (P<0,01) from P2X7-WT. These are Leu33Ala ( $\tau_{\text{slow}} = 9,91 \pm 2,12$  s) and Val41Ala ( $\tau_{\text{slow}} = 29,05 \pm 11,43$  s). Three other mutations differed with lower statistical significance (P<0,05), these being Gly27Ala ( $\tau_{\text{slow}} = 8,37 \pm 3,4$  s), Phe38Ala ( $\tau_{\text{slow}} = 9,66 \pm 4,72$ s) and Ser47Ala ( $\tau_{\text{slow}} = 9,28 \pm 4,18$  s) (Fig. 4.5).

Two mutations differed with high statistical significance (P<0,01) in  $\tau_{\text{fast}}$ . These are Trp31Ala ( $\tau_{\text{fast}} = 0,45 \pm 0,1$ s) and Val41Ala ( $\tau_{\text{fast}} = 1,1 \pm 0,08$  s). Gly27Ala ( $\tau_{\text{fast}} = 0,25 \pm 0,05$ s) and Phe38Ala ( $\tau_{\text{fast}} = 0,78 \pm 0,08$  s) differed from P2X7-WT as well, but with less statistical significance (P<0,05) (Fig. 4.5).

In the contribution of  $\tau_{\text{fast}}$  parameter, only Val41Ala (contribution of  $\tau_{\text{fast}} = 64,39 \pm 4,19\%$ ) differed with high statistical significance (P<0,01) from P2X7 WT. Two other mutations, Leu33Ala (contribution of  $\tau_{\text{fast}} = 65,58 \pm 5,96\%$ ) and Ser39Ala (contribution of  $\tau_{\text{fast}} = 64,92 \pm 6,35\%$ ) differ as well, but with lower statistical significance (P<0,05). (Fig. 4.5)

The number of cells that was used for this analysis is as follows: Gly27Ala (n=6 cells), Trp31Ala (n=12 cells), Leu33Ala (n=9 cells), Phe38Ala (n=7 cells), Ser39Ala (n=8 cells), Val41Ala (n=6 cells) and Ser47Ala (n=5 cells).

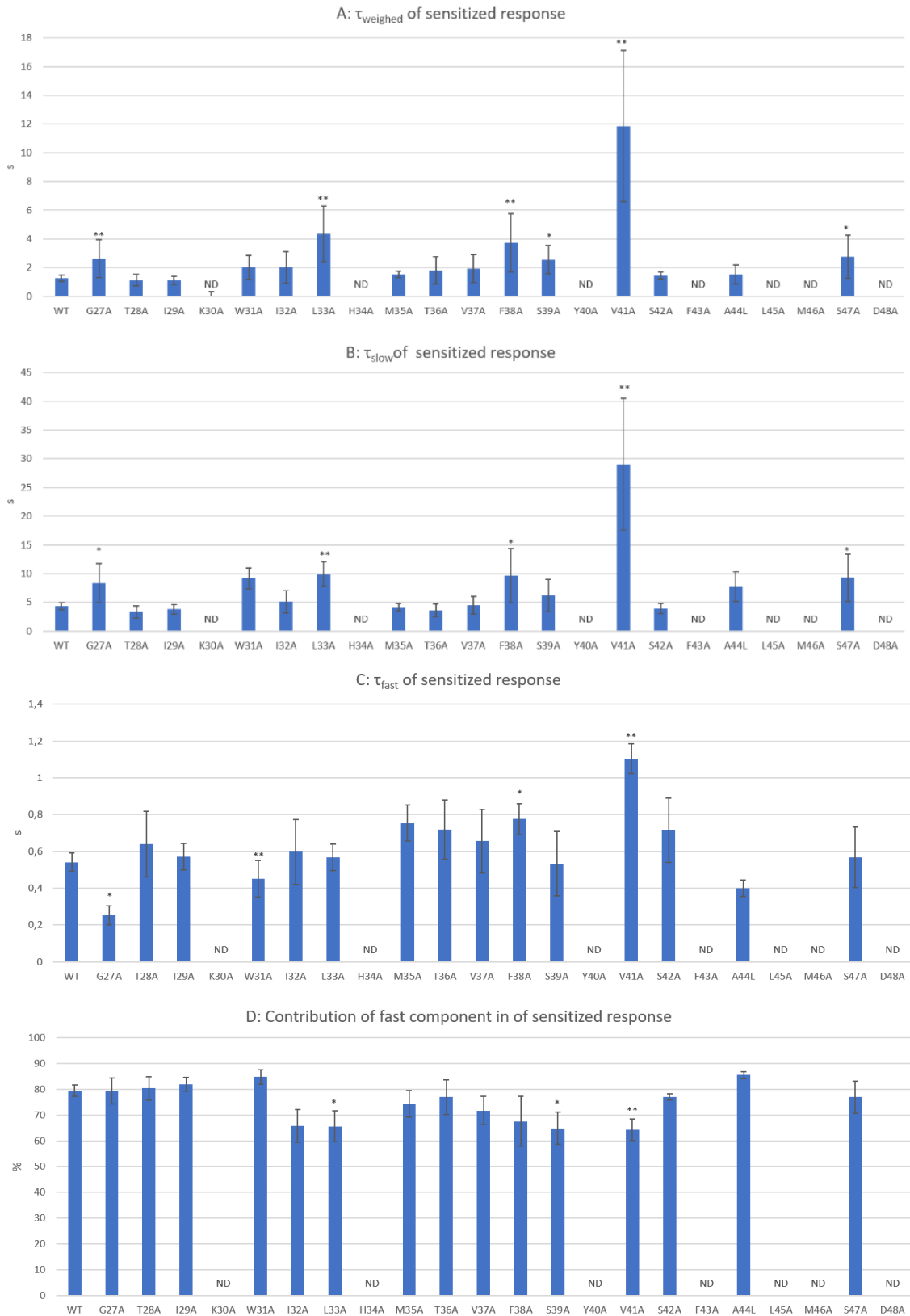


Figure 4.5: Effect of mutation of TM1-P2X7 residues on  $\tau_{\text{weight}}$  (A),  $\tau_{\text{slow}}$  (B),  $\tau_{\text{fast}}$  (C) and contribution of  $\tau_{\text{fast}}$  (D) values in sensitized responses after prolonged 100 $\mu$ M BzATP stimulation. (\*\*) indicates statistically highly significant ( $P < 0,01$ ) difference between P2X7-WT and mutant and (\*) indicates statistically significant ( $P < 0,05$ ) difference between P2X7-WT and mutant as determined by unpaired t-test. ND = not determined.

## 4.2. Microfluorometric measurements:

Microfluorimetric measurement of ethidium bromide uptake was performed for mutations that showed statistically significant ( $P < 0,01$ ) differences from P2X7-WT in  $\tau_{\text{weight}}$ , either in naïve or sensitized state. These mutations are Gly27Ala, Trp31Ala, Leu33Ala, Thr36Ala, Phe38Ala and Val41Ala. Accumulation of ethidium bromide by HEK293T cells expressing P2X7-WT or selected TM1 mutants was also measured in naïve and sensitized state of receptor. When measuring the naïve uptake, the cells were perfused with 20  $\mu\text{M}$  ethidium bromide solution for 30s, and then solution containing 20  $\mu\text{M}$  ethidium bromide and 100  $\mu\text{M}$  BzATP was applied for 60s. When the uptake was measured in sensitized state, the cells were perfused first with 100 $\mu\text{M}$  BzATP solution for 60 s to sensitize the receptor. Then the agonist was washed out via 60 s long application of ECS. Afterwards, 20  $\mu\text{M}$  ethidium bromide solution was applied for 30 s, followed by application of solution containing 20  $\mu\text{M}$  ethidium bromide and 100 $\mu\text{M}$  BzATP for 60 s. The increase in fluorescence as a measure of ethidium bromide uptake was examined 40 s after 100 $\mu\text{M}$  BzATP application in the presence of ethidium bromide (Fig. 4.6).

Ethidium bromide uptake by cells with sensitized P2X7-WT was always significantly ( $P < 0,01$ ) higher compared to cells expressing P2X7-WT in naïve state ( $n=6$  experiments, each with 20 to 40 cells)

Two mutations, Thr36Ala and Val41Ala, showed statistically significant ( $P < 0,05$ ) increase of ethidium bromide accumulation in sensitized state, comparable with the increase observed in P2X7-WT receptor.

The uptake by cells expressing Val41Ala was, however, very low, both in naïve and sensitized states. Mutation Trp31Ala showed a tendency to increase ethidium bromide uptake in sensitized state, but it was not statistically significant. Cells expressing mutations Gly27Ala, Leu33Ala or Phe38Ala did not show increase in ethidium bromide uptake in sensitized state of receptor. Moreover, mutation Phe38Ala even showed a highly statistically significant ( $P < 0,01$ ) decrease in ethidium bromide uptake after sensitization.

The number of experiments per mutant was as follows: Gly27Ala ( $n=1$  experiment; 11 naïve cells; 11 sensitized cells), Trp31Ala ( $n=1$  experiment; 41 naïve cells; 45 sensitized cells), Leu33Ala ( $n=1$  experiment; 32 naïve cells; 27 sensitized cells), Thr36Ala ( $n=1$  experiment; 43 naïve cells; 30 sensitized cells), Phe38Ala ( $n=1$  experiment; 63 naïve cells; 74 sensitized cells), Val41Ala ( $n=1$  experiment; 27 naïve cells; 23 sensitized cells).

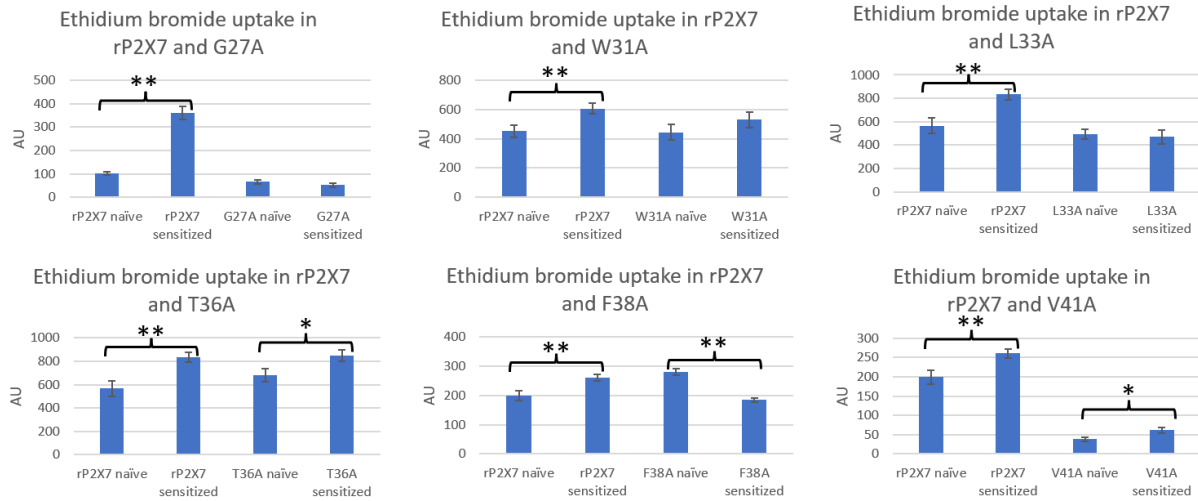


Figure 4.6. Summary histograms showing ethidium bromide uptake by cells expressing naïve and sensitized receptors (in arbitrary units, AU). Selected mutants were measured simultaneously with P2X7-WT in all experiments. (\*\*) indicates statistically highly significant ( $P < 0,01$ ) difference between naïve and sensitized state (\*) indicates statistically significant ( $P < 0,05$ ) difference between naïve and sensitized state.

## 5. Discussion

Alanine or leucine mutations of amino acids within the TM1 domain of rat P2X7 receptor were examined using electrophysiological and microfluorimetric methods with the aim to identify residues that play a key role in deactivation kinetics and dye uptake function. Compared to P2X7-WT, significantly different deactivation properties were observed for Gly27Ala, Trp31Ala, Leu33Ala, Thr36Ala, Phe38Ala and Val41Ala mutants, and all but one, Thr36Ala, exhibited also significant changes in ethidium bromide uptake indicating that changes in P2X7 deactivation impact on function that follow receptor activation such as dye accumulation. Significant change in contribution of fast component was also observed for naive Thr28Ala compared to P2X7-WT, but its impact on dye uptake function was not investigated.

*General characterization of P2X7 deactivation with regards to aims of the study:* Current decay of P2X7-WT and TM1 mutants was described by a biexponential function. This is in partial agreement with other P2X7 study showing that biexponential decay could be observed at high concentrations of agonist (Yan et al., 2010). Biexponential fitting showed that there are two kinetically distinct mechanisms of P2X7 deactivation that can be characterized by  $\tau_{fast}$  and  $\tau_{slow}$ , in both naïve and sensitized states of the receptor. After prolonged agonist stimulation, sensitized P2X7-WT showed significantly increased  $\tau_{fast}$ , but  $\tau_{slow}$  was not changed significantly. This could indicate that fast component of the biexponential decay is controlled by agonist unbinding which is slower in receptor exhibiting higher affinity for agonist, while the mechanism of the slow component is affected by other processes. The underlying mechanism is still unknown

*Nonfunctional mutations:* It is important to note that several TM1 mutations could not be properly examined electrophysiologically, as the currents amplitude elicited by BzATP application was very low, reaching few pA or tens of pA. These mutations are: Lys30Ala, His34Ala, Tyr40Ala, Phe43Ala, Leu45Ala, Met46Ala and Asp48Ala. It was not possible to evaluate their deactivation time constants, since the BzATP-induced responses were indistinguishable from basal electrical noise of the cell itself. One possible explanation was that alanine substitution of these residues prevented membrane expression of P2X7 protein in the membrane. Recent yet unpublished study examined cell surface expression of these nonfunctioning mutations (Rupert et al., submitted). All nonfunctional mutations, with exception of Asp48A, were found to have their membrane expression/total expression ratio statistically significantly lower compared to P2X7-WT (Fig.5.1). Therefore, the authors of

this study concluded that impaired receptor trafficking was the main reason for low amplitude of BzATP-induced current observed in these mutations. Interestingly, Gly27Ala mutation

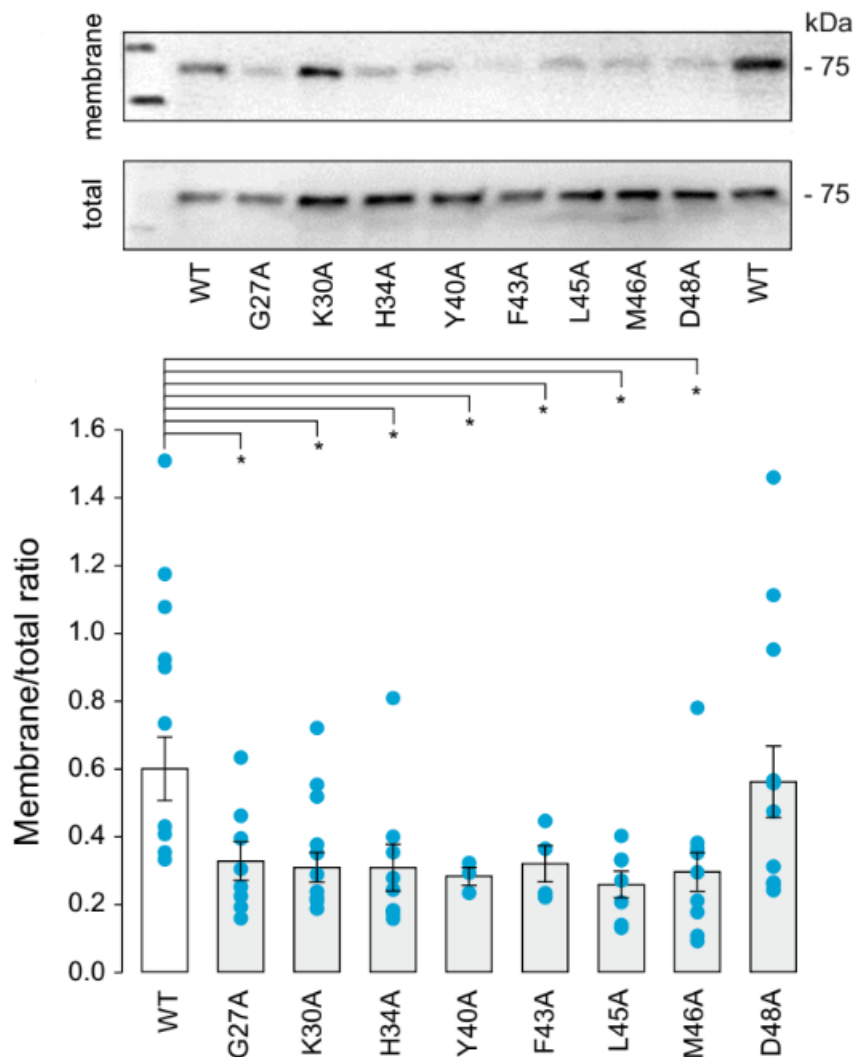


Figure 5.1: Depiction of membrane/total ratio of P2X7-WT and the TM1 mutations. “\*” signifies a difference from P2X7-WT as found by (Rupert et al., submitted), Taken and adjusted from (Rupert et al., submitted).

exhibited significantly lower membrane expression but its deactivation properties could be measured, indicating that alanine substitution of Gly27 affects P2X7 in two ways: it decreases surface expression of P2X7 protein and markedly slows channel deactivation kinetics. It might also be important to note, that K30A mutation was recently observed to impair interaction of paxillin with P2X7 is promoted upon ATP stimulation (Wang et al., 2020). The reason for the impaired interaction of K30A with paxillin could be due to the non-functionality of this mutation observed here. Mutations of TM1 domain of P2X7 that showed significantly different deactivation behavior, and possible reasons for these changes will now be discussed.

*Gly27Ala*: Glycine 27, positioned at the cytoplasmic end of TM1 of the P2X7 receptor is very well conserved among all other P2X receptors. This conservation among the P2X receptor family might suggest an important role of this particular amino acid. Glycine is often considered to play a role of a sort of a “hinge” in proteins, because of small size of this amino acid residue (Doyle, 2004; Khakh & Alan North, 2006). Deactivation of naïve *Gly27Ala* response was significantly different from that of naïve P2X7-WT, so that  $\tau_{\text{weight}}$  of *Gly27Ala* was almost four times higher than that of P2X7-WT. Even though naïve *Gly27Ala* responses differ in all three parameters that were followed ( $\tau_{\text{slow}}$ ,  $\tau_{\text{fast}}$  and contribution of fast component), the greatest change that was responsible for that  $\tau_{\text{weight}}$  changes was observed in the contribution of fast component, which was significantly lower in G27A compared to P2X7-WT. In other words, it means that the contribution of slow component in G27A increased compared to P2X7-WT.

A notable shift in the *Gly27Ala* deactivation behavior was observed by comparing the naïve and sensitized response. The sensitized response is prolonged as well, compared to P2X7-WT, but the usual sensitization-induced change in contribution of fast component is absent. The ethidium bromide uptake experiments showed that dye uptake was inhibited in both naïve and sensitized *Gly27Ala*. These data indicate an important role of Gly27 in P2X7 deactivation dynamics induced by prolonged agonist stimulation.

Molecular 3D model of rat P2X7 shows that glycine 27 is located in close proximity to N-terminus (McCarthy et al., 2019). It is located near the N-terminal strand that is part of the stable P2X7 cytoplasmic cap, which is considered to be a key feature of P2X2 and P2X7 receptor's ability not to undergo desensitization (Mansoor et al., 2016; McCarthy et al., 2019). It could therefore be hypothesized that Gly27 functions as a hinge that could affect the channel gating by allowing movement of TM1  $\alpha$ -helix and interaction of TM1 amino acids with the cytoplasmic cap on N-terminus. Thus, alanine substitution of Gly27 could lead to limitations in this movement and interactions which impacted on dye uptake function of P2X7.

The increase in contribution of slow component to deactivation observed in naïve *Gly27Ala* mutation compared to naïve WT could be explained either by impairment of receptor trafficking, which was observed for this mutant (Figure 5.1), or by impairment of the gate closure itself. Thus, alanine substitution of Gly27 could also affect the conformation shift from ligand-bound open state to closed-apo state of P2X7.

After sensitization, the contribution of slow component to Gly27Ala receptor deactivation is decreased compared to naïve state and the average contribution of fast component is very similar to that of P2X7-WT. It could be explained by more intensive receptor trafficking after sensitization (i.e. receptor externalization) or association of the receptor with another molecule, that could perhaps induce more “WT-like” behavior of this mutants in terms of open to closed conformation shift. Possible P2X7 interplay with other membrane molecules, that affects P2X7 channel characteristics, was already observed (Dunning et al., 2021; Moura et al., 2015).

*Trp31Ala*: Aromatic amino acids in first transmembrane domain are well known to be important for function of all P2X receptors in general, as was previously observed by several studies (Haines et al., 2001; Jelínková et al., 2008; Li et al., 2004; Jindrichova et al., 2010). On the other hand, tryptophan 31 is specific for P2X7, other P2X subtypes contain arginine at the position corresponding to Trp31. Arginine has very different chemical properties (it is a positively charged residue), and therefore it probably serves very different roles in these receptors.

Characteristics of the Trp31Ala naïve response deactivation are significantly different from that of P2X7-WT. Deactivation time constant  $\tau_{\text{weight}}$  of naïve Trp31Ala response was significantly higher compared to that naïve P2X7-WT, which was due to significantly reduced contribution of fast deactivation component to current decay. However, after prolonged stimulation, only one parameter was significantly different. This was fast deactivation time constant,  $\tau_{\text{fast}}$ , which was slightly but significantly lower compared to that of sensitized WT receptor. The Trp31Ala mutation was found to exhibit no significant changes in  $EC_{50}$  after stimulation compared to WT receptor (Rupert et al., submitted). This could indicate that the value of fast deactivation time constant is lower compared to that of sensitized WT because the Trp31Ala is not able to sensitize properly. In agreement with this idea, Trp31Ala showed only slight increase in ethidium bromide uptake when pre-sensitized by application of BzATP compared to ethidium bromide uptake by receptor in naïve state.

Another aromatic amino acids, tyrosine residues located in intracellular N- and C-termini in close proximity to transmembrane domains, were observed to effect cholesterol-induced modulation of P2X receptors (Robinson et al., 2014b). Currents mediated by P2X7 receptors are known to be potentiated upon cholesterol depletion and ethidium bromide uptake is increased when the cell membrane is treated by cholesterol chelating agents (Robinson et al., 2014b). However, this study also showed that cholesterol-induced inhibition of P2X7 receptor persists in construct lacking both N- and C-termini. It indicates that even

though cholesterol recognition amino acid consensus motifs were found in N- and C-termini, transmembrane domains themselves, TM2 and particularly TM1 which has more extensive contacts with the membrane lipids, also play important role in cholesterol sensing and aromatic Trp31 could theoretically be involved. Modulation of P2X receptor behavior by membrane lipids was also observed in other studies (Dunning et al., 2021; Karasawa et al., 2017). In addition, several non-polar amino acids in TM1 domain were also indicated to have a role in ivermectin binding to P2X4 receptor (Jelínková et al., 2008). Ivermectin is a large lipophilic molecule that also acts as a positive allosteric modulator on human P2X7 (Nörenberg et al., 2012) and its interaction with non-polar amino acids in TM1 domain of human P2X7 receptor is highly probable.

Tryptophan 31, according to the cryo-EM structures of P2X7 receptor (McCarthy et al., 2019), is in relatively close proximity to residues in N-termini of cytoplasmic cap. In particular, Val10 is located in such manner, so that the distance between Trp31 and Val10 of neighboring subunit is less than 4Å for several atoms of Val10 residue (Fig. 5.2). The proximity can be observed both in closed-apo state and open-ATP bound state of the P2X7 receptor. This could indicate a possible hydrophobic interaction between Trp31 and Val10 of two neighboring subunits (Fig. 5.2). Alanine substitution of Trp31 might therefore impair this potential interaction of cytoplasmic cap with TM1 domain, which may be the reason for the changes observed in Trp31Ala behavior. Mutations of threonine 15 in the cytoplasmic cap have been also shown to impair deactivation properties of P2X7 (Yan et al., 2010).

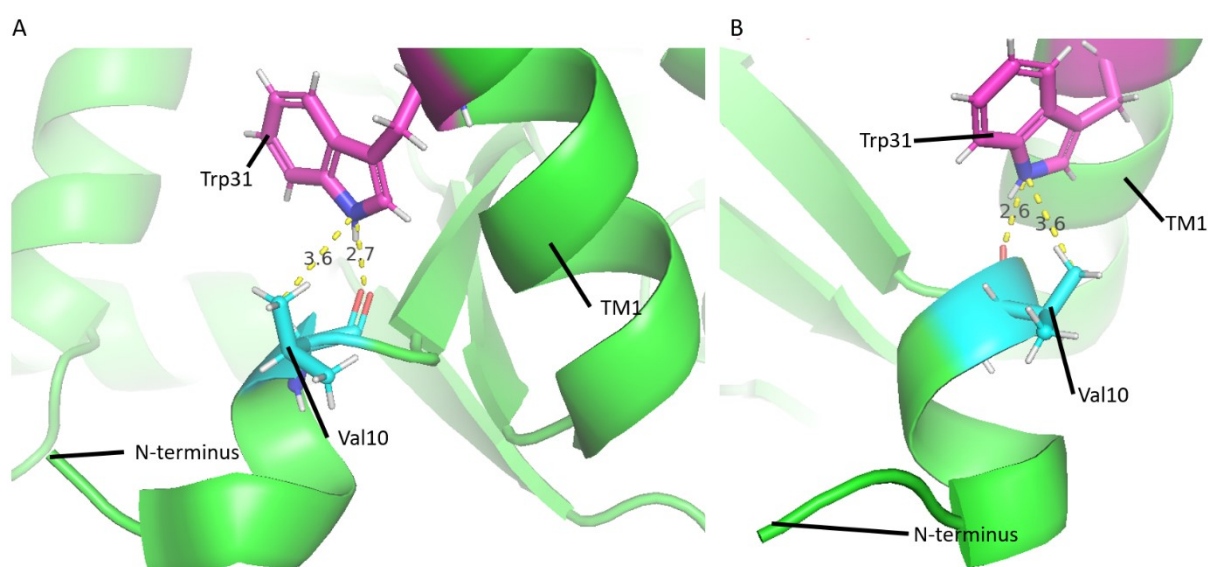


Figure 5.2: Depiction of Trp31 (in magenta) position and its proximity to Val10 (turquoise) in ATP bound-open (A) and apo-closed (B) state. The values shown are in Å, the structure models (rP2X7) used are 6u9w (A) and 6u9v (B) in PDB.

*Leu33Ala*: Leucine is an amino acid with a non-polar residue and even though alanine is also non-polar, it is much smaller, and consequently significant changes in deactivation were observed for the *Leu33Ala* mutant. Particularly, increase in  $\tau_{\text{slow}}$ ,  $\tau_{\text{fast}}$  and  $\tau_{\text{weight}}$  and decrease in fast component contribution was observed in naïve *Leu33Ala* response. After *Leu33Ala* sensitization, deactivation time constants  $\tau_{\text{slow}}$  and  $\tau_{\text{weighed}}$  remained increased compared to sensitized P2X7-WT, but fast component did not increase further. In general, *Leu33Ala* mutation does not change deactivation characteristics very much after sensitization, most probably because its deactivation is highly elongated already in native state. This is in agreement with the microfluorimetric results, where no significant increase in ethidium bromide uptake was observed after pretreatment with agonist. This could indicate that sensitization-induced changes causing increase in ethidium bromide uptake function, that readily occur in P2X7-WT receptor, do not occur in *Leu33Ala* mutation possibly because maximal limit for dye uptake rate was already reached in naive mutation.

The non-polar character of leucine could indicate similar role of Leu33 to that previously discussed for Trp31. It means that Leu33 could play a role in binding of lipophilic molecules, such as cholesterol or membrane phospholipids which are known to affect P2X7 channel biophysical characteristic. Leucine can generally be involved in cholesterol binding to membrane proteins (Murrell-Lagnado et al., 2017). These possible interactions could therefore explain difference in *Leu33Ala* deactivation kinetics since interaction with lipids is crucial for P2X7 channel function (Karasawa et al., 2017). However, according to the model of rat P2X7 receptor (Fig. 5.3) residue Leu33 is not oriented directly to the membrane and might not be as exposed to membrane lipids as other hydrophobic amino acids in P2X7-TM1 domain (McCarthy et al., 2019).

Another potential clue explaining the behavior of *Leu33Ala* could be also found in 3D structures of P2X7 receptor (McCarthy et al., 2019). Even though Leu33 does not directly face TM2 domain, two TM2 amino acids can be found in its vicinity. The distance between Leu33 and Leu346 or Ala347 in TM2 are smaller than 4Å in both apo-closed state and ATP bound-open state of the receptor (Fig. 5.3). Both these amino acids are non-polar and such proximity could then indicate a possible hydrophobic interaction between two transmembrane domains, TM1 and TM2, of the same subunit which could stabilize their position in the membrane. It is also important to note, that all P2X receptors contain a non-polar residue, valine, leucine, or isoleucine, at this position of TM1, and P2X7 receptors of other species contain either isoleucine phenylalanine on this position. This conservation of non-polarity at this particular position could possibly indicate its importance for hydrophobic interaction

between transmembrane helices also for other P2X receptors. Even though alanine is also non-polar residue, the shorter length of its side chain could perhaps cause insufficient interaction with residues of TM2 and thus impair the receptor function (Fig. 5.3).

In addition, TM2 amino acids indicated to participate in binding of ivermectin to transmembrane domain of P2X4, namely Ala349 (rP2X4 numbering), correspond to Ala347 in rP2X7, which could support the possible lipophilic molecule interaction in this area of the P2X7 receptor (Jelínková et al., 2008).

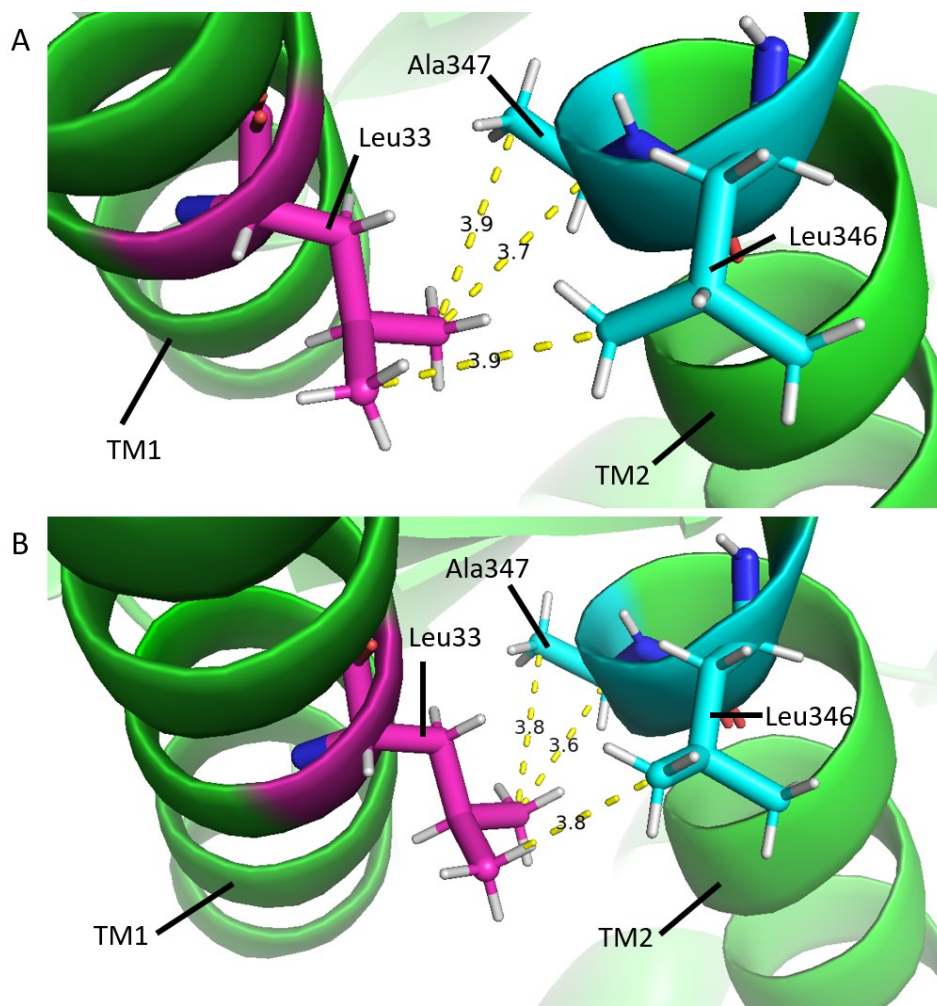


Figure 5.3: Depiction of Leu33 (in magenta) position and its proximity to Leu346 and Ala347 (turquoise) in ATP bound-open (A) and apo-closed (B) state. The values shown are in Å, the structure models (rP2X7) used are 6u9w (A) and 6u9v (B) in PDB.

*Thr36Ala*: Threonine is relatively small amino acid with relatively short, uncharged, polar residue. Significant difference in deactivation of Thr36Ala compared to that of P2X7-WT receptor was observed only in naïve response and only the  $\tau_{\text{weighed}}$  was increased, but not as dramatically as in other P2X7 mutations discussed above. This indicates, that Thr36Ala

behaves quite similarly to P2X7-WT when sensitized, but the behavior is changed for naïve receptor. Similar WT-like behavior of Thr36Ala was also observed in microfluorimetric measurements of ethidium bromide uptake, which was significantly increased after receptor sensitization.

Other rat P2X subtypes contain amino acids with non-polar character at position corresponding to Thr36, such as leucine or valine, with exception of the non-functional P2X6, that contains glycine. Non-polar residues can be found at position 36 even among P2X7 receptors of other species, such as human, panda or canines, where leucine or valine are present. In general, this could indicate that polar residue at this position is not crucial for P2X receptor function but might play a role in rat P2X7.

According to the rat P2X7 receptor model, Thr36 residue does not face the TM2 of the same subunit, nor is it fully oriented towards the membrane, but could possibly be exposed to molecules within the membrane even more than the previously discussed Leu33, for example. Therefore, the Thr36 does not seem to have possible interacting partners within the receptor itself, but its position might allow to interact with membrane lipids or other molecules present within the membrane (McCarthy et al., 2019).

The polar nature of this residue might exclude any sort of hydrophobic interaction, which is typically implicated for cholesterol recognition amino acid consensus motifs. Thus Thr36 could serve other roles. Theoretically it could function to prevent or impair interaction of TM1 helix with other membrane proteins, if present. The more profound change in deactivation kinetics observed in naïve Thr36Ala response could therefore theoretically be explained by possible interaction of Ala36 with membrane lipids which is otherwise absent in WT receptor containing Thr36. In sensitized Thr36Ala, this interaction of alanine with lipophilic molecules does not play a role, and it is a reason why this mutant exhibited WT-like behavior. This idea is supported by many studies showing that other membrane proteins are important, but not crucial, for regulation of P2X7 function (Dunning et al., 2021; Karasawa et al., 2017; Moura et al., 2015).

*Phe38Ala*: Alanine substitution of phenylalanine at position 38 was observed to change significantly deactivation behavior mainly in sensitized state. Compared to sensitized P2X7-WT, mutation Phe38Ala showed significant increases in  $\tau_{\text{weight}}$ ,  $\tau_{\text{fast}}$  and  $\tau_{\text{slow}}$ , accompanied by reduced contribution of fast component to deactivation. In naïve state, the Phe38Ala responses differed from P2X7-WT only in the  $\tau_{\text{fast}}$  parameter which was increased, and other parameters were not changed. This indicates that changes in deactivation behavior of this

mutation are similar to those found for Thr36Ala mutation, where differences in deactivation kinetics were observed also only for sensitized receptor compared to P2X7-WT. In contrast to Thr36Ala, mutation Phe38Ala was not observed to increase ethidium bromide uptake after receptor sensitization. The uptake was actually significantly decreased after sensitization receptor compared to P2X7-WT, which could indicate an importance of this residue for changes that follow receptor sensitization.

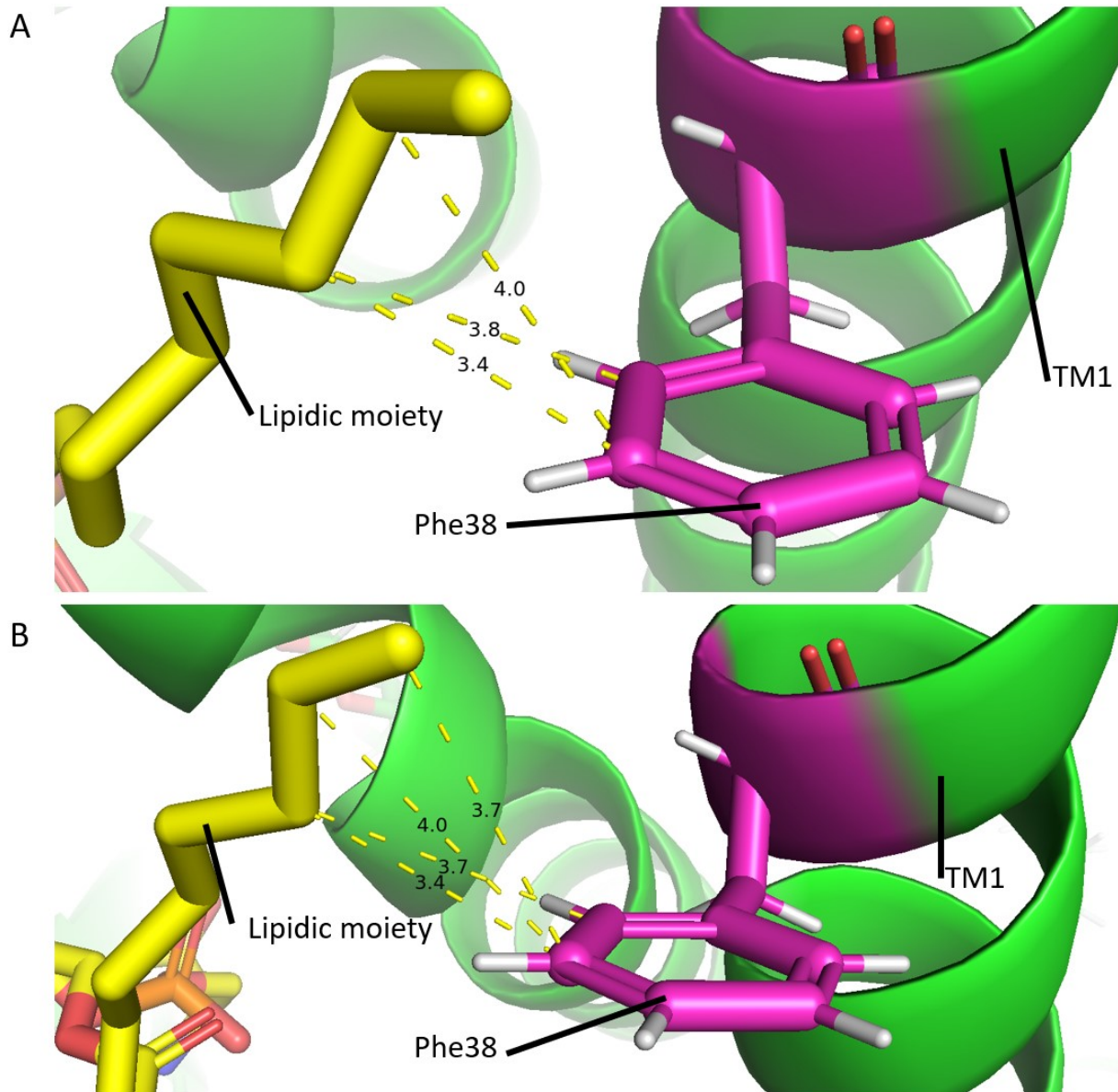
Phenylalanine 38 belongs to aromatic amino acids which are generally considered to be important for P2X receptor function, and could therefore be important for rat P2X7 receptor function as well. This could be supported by the fact, that human and panda P2X7 receptors both contain phenylalanine at position 38. Canine P2X7 receptor and other rat P2X subtypes also contain an amino acid with a non-polar residue at this position, such as valine, leucine, isoleucine or even alanine. This could point towards conservation of non-polarity at this position, with the notable exception of most other P2X7 receptors, where non-polarity as well as aromaticity is present.

In the rat P2X7 3D model, Phe38 is located in the upper part of the TM1 helix, with its residue not facing either to the receptor axis nor directly away from it and into the membrane (not shown). It is relatively close to TM2 domain of the same subunit, however, probably not close enough to form any sort of interaction with any of TM2 amino acids. Therefore, any possible inter- or intra-receptor interaction with Phe38 probably does not exist both in apo-closed and ATP bound-open states of the rat P2X7 receptor.

However, according to the 3D structures, a possible interaction of Phe38 and the lipidic moiety, inserted between transmembrane domains of neighboring subunits, can be observed in both apo-closed and ATP bound-open states of rat P2X7, since the distances between Phe38 and lipidic moiety are lower than 4Å (Fig. 5.4) (McCarthy et al., 2019). This could potentially implicate Phe38 not only as lipid interacting residue, which could be important for regulation of P2X7 function, but possibly as a residue involved in the phosphatidylserine transfer and the presumable flippase activity of P2X7 (McCarthy et al., 2019).

*Val41Ala:* Both valine and alanine are small amino acids with non-polar character. It is therefore surprising that Val41Ala is significantly different from P2X7-WT in all deactivation characteristics that were evaluated. In addition to prolongation of all deactivation time constants in both naïve and sensitized state, ethidium bromide uptake by cells expressing Val41Ala was severely reduced, reaching only several tens of AU. Upon sensitization, the

ethidium bromide uptake function of Val41Ala was increased, but still remained significantly reduced compared to sensitized P2X7-WT. With respect to the fact that physicochemical



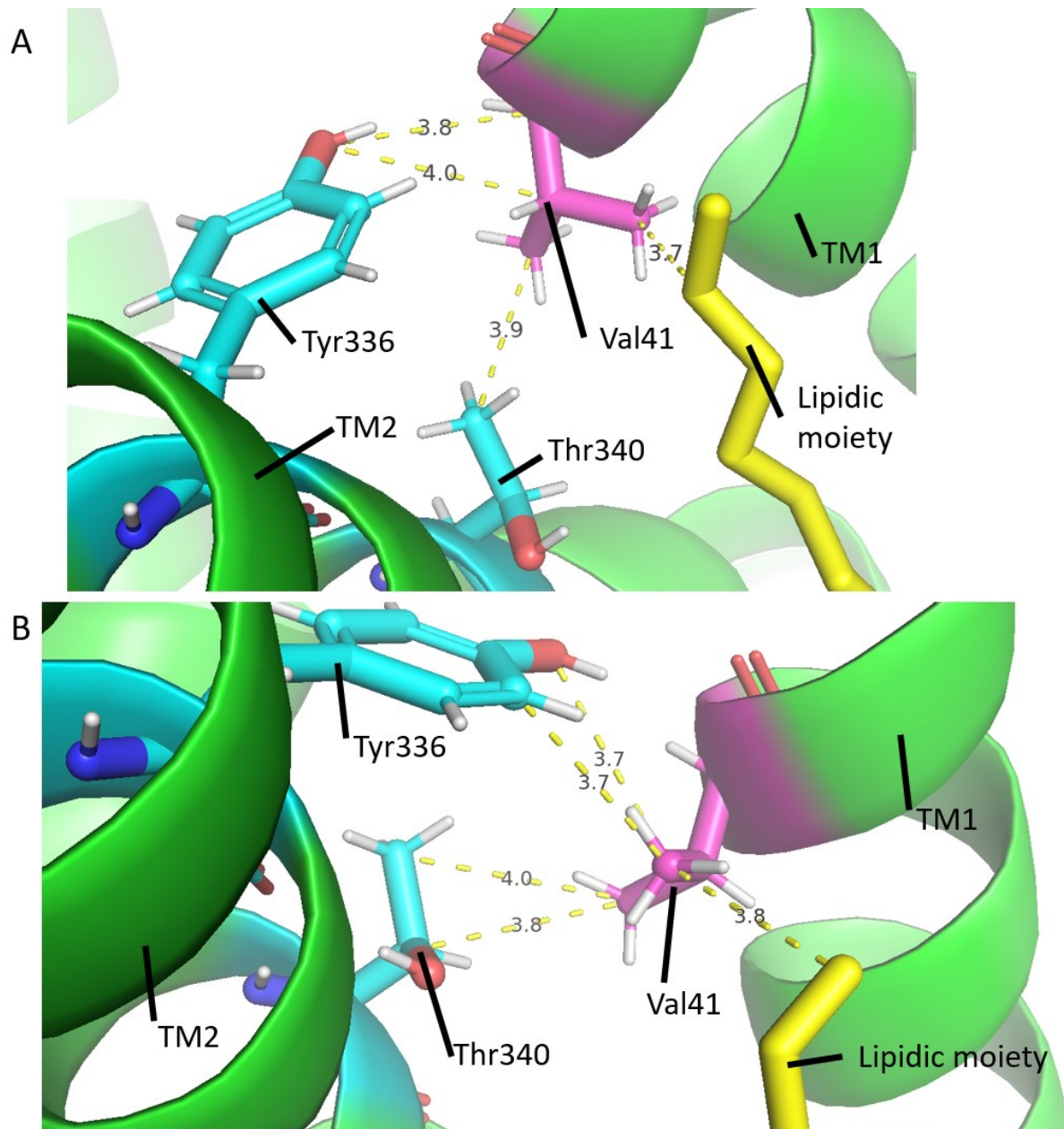
Depiction of Phe38 (in magenta) position and its proximity to the lipidic moiety (yellow) in ATP bound-open (A) and apo-closed (B) state. The values shown are in Å, the structure models (rP2X7) used are 6u9w (A) and 6u9v (B) in PDB.

properties of valine and alanine are very similar, this could indicate, that other factor contribute to the observed changes in addition to alanine substitution.

Other rat P2X subtypes and P2X7 receptors of other species also contain non-polar amino acid at position 41, usually valine, leucine or isoleucine, and the P2X2 and P2X3 contain phenylalanine at this position. However, Val41 is adjacent to conserved tyrosine 40 (rP2X7 numbering). Tyrosine 40 is conserved among all P2X receptors and its mutation has

severe impact on P2X function, which was observed also in rat P2X7, as was mentioned above (Jindrichova et al., 2010). This can possibly lead to the conclusion, that Val41 is important for receptor function perhaps because of its proximity to Tyr40, and that alanine substitution of Val41 causes disturbance in the surrounding of the Tyr40 that could induce serious impairment of P2X7 function.

However, the 3D structures of rat P2X7 shows that Val41 faces directly towards receptor axis and TM2 (Fig.5.5). At this place, there are several important residues in the



TM2 domain that Depiction of Val41 (in magenta) position and its proximity to the lipidic moiety (yellow) and to Tyr336 and Thr340 (turquoise) in ATP bound-open (A) and apo-closed (B) state. The values shown are in Å, the structure models (rP2X7) used are 6u9w (A) and 6u9v (B) in PDB.

are important for P2X7 function, including Thr340 and to Tyr336 (McCarthy et al., 2019; Pippel et al., 2017). In the apo-closed state of the rat P2X7 structure, Val41 is closer than 4Å to Thr340 and to Tyr336. Both of these amino acids are very close to what is considered pore gate of P2X7 receptor, that is located between Ser339 and Ser342 (McCarthy et al., 2019; Pippel et al., 2017). In the ATP bound-open state of the receptor, similar distances can be found between Val41 and Tyr336, however, Thr340 is moved further than 4Å from the Val41. The observed profound changes in deactivation and dye uptake function of Val41Ala thus could be also attributed to disturbance in the surrounding of the gate that could induce serious impairment of P2X7 function and/or impair the stability of TM2 helix in apo-closed state of the receptor.

Additional insight into the role of Val41 can be gained from the observed proximity of Val41 to one of the tails of the lipidic moiety inserted between the two neighboring subunits' TM1 and TM2 (Fig.5.5). Valine 41 can be observed in proximity of this molecule in both apo-closed and ATP bound-open states and could thus be implicated to have a similar putative role as suggested previously for Phe38, emphasizing lipid interaction and possible role in phosphatidylserine exposure.

## 6. Conclusion

Alanine substitution of all residues discussed above led to changes of deactivation kinetics and impairment of dye uptake function of rat P2X7. Some of these residues, such as Leu33 or Val41 could theoretically interact with TM2 of the same subunit, and abolition or impairment of such interaction by alanine substitution could lead to the observed phenotype, as interaction of TM1 and TM2 was theorized to occur and affect P2X receptor. It might be interesting and potentially supporting this hypothesis, if residues in TM2 domain of P2X7, that are implied to interact with Leu33 and Val41, were also substituted for alanine, as they could perhaps yield a similar deactivation phenotype provided that TM1 and TM2 interaction occur at these sites.

Trp31 and Phe38 are both aromatic residues, which are in general considered to be important for P2X receptor function. Therefore, the impairment of receptor function in Trp31Ala and Phe38Ala mutations might not be surprising. Trp31, along with Gly27, that is thought to serve as a hinge at the N-terminal end of TM1, are in close proximity to cytoplasmic cap formed by N-terminal strand of neighboring subunit, where they could also affect the TM1 to TM2 interaction and receptor phenotype. However, molecular model of P2X7 shows that the role of Phe38 might not be due to its aromatic character.

Tryptophan, leucine and valine are all amino acids known for their importance in binding of membrane lipids. Trp31, Leu33 and Val41 could be involved in cholesterol interaction which is known to be important for P2X7 signaling and is known to occur in transmembrane domain. Perhaps binding of lipophilic molecule could involve both TM1 and TM2 as it was found for lipophilic ivermectin which acts as positive allosteric modulator not only in P2X4, but also P2X7 of some species. It could provide useful insight into role of these residue if their alanine substitutions are examined for their possible role in cholesterol and/or ivermectin binding.

Lastly, Phe38 and Val41 are in close proximity of the lipidic moiety discovered in the cryo-EM structure of rat P2X7. This moiety could, according to the authors of this study, represent phosphatidylserine bound between TM1 and TM2. This could then imply that Phe38 and Val41 might have a role in flippase activity of the receptor. Phe38Ala and Val4Ala could be tested for their impact on phosphatidylserine translocation to solidify the potential role of TM1 and TM2 in this process.

## 7. References

- Abbracchio, M. P., Burnstock, G., Verkhratsky, A., & Zimmermann, H. (2009). Purinergic signalling in the nervous system: an overview. *Trends in Neurosciences*, 32(1), 19–29. <https://doi.org/10.1016/j.tins.2008.10.001>
- Adinolfi, E., Cirillo, M., Woltersdorf, R., Falzoni, S., Chiozzi, P., Pellegatti, P., ... Di Virgilio, F. (2010). Trophic activity of a naturally occurring truncated isoform of the P2X7 receptor. *The FASEB Journal*, 24(9), 3393–3404. <https://doi.org/10.1096/fj.09-153601>
- Allsopp, R. C., & Evans, R. J. (2015). Contribution of the juxtatransmembrane intracellular regions to the time course and permeation of ATP-gated P2X7 Receptor Ion Channels. *Journal of Biological Chemistry*, 290(23), 14556–14566. <https://doi.org/10.1074/jbc.M115.642033>
- Andrejew, R., Oliveira-Giacomelli, Á., Ribeiro, D. E., Glaser, T., Arnaud-Sampaio, V. F., Lameu, C., & Ulrich, H. (2020). The P2X7 Receptor: Central Hub of Brain Diseases. *Frontiers in Molecular Neuroscience*, 13(July), 1–27. <https://doi.org/10.3389/fnmol.2020.00124>
- Anselmi, F., Hernandez, V. H., Crispino, G., Seydel, A., Ortolano, S., Roper, S. D., ... Mammano, F. (2008). ATP release through connexin hemichannels and gap junction transfer of second messengers propagate Ca<sup>2+</sup> signals across the inner ear. *Proceedings of the National Academy of Sciences of the United States of America*, 105(48), 18770–18775. <https://doi.org/10.1073/pnas.0800793105>
- Bhattacharya, A., Vavra, V., Svobodova, I., Bendova, Z., Vereb, G., & Zemkova, H. (2013). Potentiation of inhibitory synaptic transmission by extracellular ATP in rat suprachiasmatic nuclei. *Journal of Neuroscience*, 33(18), 8035–8044. <https://doi.org/10.1523/JNEUROSCI.4682-12.2013>
- Bianchi, B. R., Lynch, K. J., Touma, E., Niforatos, W., Burgard, E. C., Alexander, K. M., ... Van Biesen, T. (1999). Pharmacological characterization of recombinant human and rat P2X receptor subtypes. *European Journal of Pharmacology*, 376(1–2), 127–138. [https://doi.org/10.1016/S0014-2999\(99\)00350-7](https://doi.org/10.1016/S0014-2999(99)00350-7)
- Buell, G., Lewis, C., Collo, G., North, R. A., & Surprenant, A. (1996). An antagonist-

- insensitive P2X receptor expressed in epithelia and brain. *EMBO Journal*, 15(1), 55–62.  
<https://doi.org/10.1002/j.1460-2075.1996.tb00333.x>
- Burnstock, G., & Kennedy, C. (1985). Is there a basis for distinguishing two types of P2-purinoceptor? *General Pharmacology*, 16(5), 433–440. [https://doi.org/10.1016/0306-3623\(85\)90001-1](https://doi.org/10.1016/0306-3623(85)90001-1)
- Burnstock, G., & Kennedy, C. (2011). P2X Receptors in Health and Disease. In *Advances in Pharmacology* (1st ed., Vol. 61). <https://doi.org/10.1016/B978-0-12-385526-8.00011-4>
- Burnstock, Geoffrey. (1972). Purinergic nerves. *Pharmacological Reviews*, (24), 509–581.
- Burnstock, Geoffrey, & Verkhatsky, A. (2012). Purinergic signalling and the nervous system. In *Purinergic Signalling and the Nervous System* (Vol. 9783642288).  
<https://doi.org/10.1007/978-3-642-28863-0>
- Cavarelli, J., Eriani, G., Rees, B., Ruff, M., Boeglin, M., Mitschler, A., ... Moras, D. (1994). The active site of yeast aspartyl-tRNA synthetase: Structural and functional aspects of the aminoacylation reaction. *EMBO Journal*, 13(2), 327–337.  
<https://doi.org/10.1002/j.1460-2075.1994.tb06265.x>
- Cheewatrakoolpong, B., Gilchrest, H., Anthes, J. C., & Greenfeder, S. (2005). Identification and characterization of splice variants of the human P2X7 ATP channel. *Biochemical and Biophysical Research Communications*, 332(1), 17–27.  
<https://doi.org/10.1016/j.bbrc.2005.04.087>
- Collo, G., North, R. A., Kawashima, E., Merlo-Pich, E., Neidhart, S., Surprenant, A., & Buell, G. (1996). Cloning of P2X5 and P2X6 receptors and the distribution and properties of an extended family of ATP-gated ion channels. *Journal of Neuroscience*, 16(8), 2495–2507.  
<https://doi.org/10.1523/jneurosci.16-08-02495>
- Colquhoun, D. (1998). Binding, gating, affinity and efficacy: The interpretation of structure-activity relationships for agonists and of the effects of mutating receptors. *British Journal of Pharmacology*, 125(5), 923–947. <https://doi.org/10.1038/sj.bjp.0702164>
- Compan, V., Ulmann, L., Stelmashenko, O., Chemin, J., Chaumont, S., & Rassendren, F. (2012). P2X2 and P2X5 subunits define a new heteromeric receptor with P2X7-like properties. *Journal of Neuroscience*, 32(12), 4284–4296.  
<https://doi.org/10.1523/JNEUROSCI.6332-11.2012>

- Courageot, M. P., Lépine, S., Hours, M., Giraud, F., & Sulpice, J. C. (2004). Involvement of sodium in early phosphatidylserine exposure and phospholipid scrambling induced by P2X7 purinoceptor activation in thymocytes. *Journal of Biological Chemistry*, 279(21), 21815–21823. <https://doi.org/10.1074/jbc.M401426200>
- Cui, W. W., Wang, S. Y., Zhang, Y. Q., Wang, Y., Fan, Y. Z., Guo, C. R., ... Yu, Y. (2022). P2X3-selective mechanism of Gefapixant, a drug candidate for the treatment of refractory chronic cough. *Computational and Structural Biotechnology Journal*, 20, 1642–1653. <https://doi.org/10.1016/j.csbj.2022.03.030>
- Cully, D. F., Vassilatis, D. K., Liu, K. K., Paress, P. S., Van Der Ploeg, L. H. T., Schaeffer, J. M., & Arena, J. P. (1994). Cloning of an avermectin-sensitive glutamate-gated chloride channel from *Caenorhabditis elegans*. *Nature*, Vol. 371, pp. 707–711. <https://doi.org/10.1038/371707a0>
- De Salis, S. K. F., Li, L., Chen, Z., Lam, K. W., Skarratt, K. K., Balle, T., & Fuller, S. J. (2022). Alternatively Spliced Isoforms of the P2X7 Receptor: Structure, Function and Disease Associations. *International Journal of Molecular Sciences*, 23(15), 1–22. <https://doi.org/10.3390/ijms23158174>
- Denlinger, L. C., Fiset, P. L., Sommer, J. A., Watters, J. J., Prabhu, U., Dubyak, G. R., ... Bertics, P. J. (2001). Cutting Edge: The Nucleotide Receptor P2X 7 Contains Multiple Protein- and Lipid-Interaction Motifs Including a Potential Binding Site for Bacterial Lipopolysaccharide . *The Journal of Immunology*, 167(4), 1871–1876. <https://doi.org/10.4049/jimmunol.167.4.1871>
- Di Virgilio, F., Schmalzing, G., & Markwardt, F. (2018). The Elusive P2X7 Macropore. *Trends in Cell Biology*, 28(5), 392–404. <https://doi.org/10.1016/j.tcb.2018.01.005>
- Ding, S., Zhu, L., Tian, Y., Zhu, T., Huang, X., & Zhang, X. (2017). P2X3 receptor involvement in endometriosis pain via ERK signaling pathway. *PLoS ONE*, 12(9), 1–17. <https://doi.org/10.1371/journal.pone.0184647>
- Donnelly-Roberts, D. L., Namovic, M. T., Surber, B., Vaidyanathan, S. X., Perez-Medrano, A., Wang, Y., ... Jarvis, M. F. (2009). [3H]A-804598 ([3H]2-cyano-1-[(1S)-1-phenylethyl]-3-quinolin-5-ylguanidine) is a novel, potent, and selective antagonist radioligand for P2X7 receptors. *Neuropharmacology*, 56(1), 223–229. <https://doi.org/10.1016/j.neuropharm.2008.06.012>

- Doyle, D. A. (2004). Structural changes during ion channel gating. *Trends in Neurosciences*, 27(6), 298–302. <https://doi.org/10.1016/j.tins.2004.04.004>
- Dunning, K., Martz, A., Peralta, F. A., Cevoli, F., Boué-Grabot, E., Compan, V., ... Grutter, T. (2021). P2x7 receptors and tmem16 channels are functionally coupled with implications for macropore formation and current facilitation. *International Journal of Molecular Sciences*, 22(12), 1–24. <https://doi.org/10.3390/ijms22126542>
- Dwyer, K. M., Kishore, B. K., & Robson, S. C. (2020). Conversion of extracellular ATP into adenosine: a master switch in renal health and disease. *Nature Reviews Nephrology*, 16(9), 509–524. <https://doi.org/10.1038/s41581-020-0304-7>
- Elena Adinolfi, Maria Giulia Callegari, Davide Ferrari, C. B., Mattia Minelli, Mariusz R. Wieckowski, Paolo Pinton, Rosario Rizzuto, A., & Virgilio, F. Di. (2005). Basal Activation of the P2X7 ATP Receptor Elevates Mitochondrial Calcium and Potential, Increases Cellular ATP Levels, and Promotes Serum-independent Growth. *Mol Biol Cell*, 16(July), 5318–5328. <https://doi.org/10.1091/mbc.e04-11-1025>
- Elsner, A., Duncan, M., Gavrilin, M., & Wewers, M. D. (2004). A Novel P2X 7 Receptor Activator, the Human Cathelicidin-Derived Peptide LL37, Induces IL-1 $\beta$  Processing and Release . *The Journal of Immunology*, 172(8), 4987–4994. <https://doi.org/10.4049/jimmunol.172.8.4987>
- Evans, R. J., Lewis, C., Virginio, C., Lundstrom, K., Buell, G., Surprenant, A., & North, R. A. (1996). Ionic permeability of, and divalent cation effects on, two ATP-gated cation channels (P2X receptors) expressed in mammalian cells. *Journal of Physiology*, 497(2), 413–422. <https://doi.org/10.1113/jphysiol.1996.sp021777>
- Feng, Y. H., Li, X., Zeng, R., & Gorodeski, G. I. (2006). Endogenously expressed truncated P2X7 receptor lacking the C-terminus is preferentially upregulated in epithelial cancer cells and fails to mediate ligand-induced pore formation and apoptosis. *Nucleosides, Nucleotides and Nucleic Acids*, 25(9–11), 1271–1276. <https://doi.org/10.1080/15257770600890921>
- Ferrari, B. D., Chiozzi, P., Falzoni, S., Hanau, S., & Virgilio, F. Di. (1997). Purinergic Modulation of Interleukin-1beta Release from Microglial Cells Stimulated with Bacterial Endotoxin. *J. Exp. Med*, 185(3), 22–25.
- Finger, T. E., Danilova, V., Barrows, J., Bartel, D. L., Vigers, A. J., Stone, L., ... Kinnamon,

- S. C. (2005). Neuroscience: ATP signalling is crucial for communication from taste buds to gustatory nerves. *Science*, *310*(5753), 1495–1499.  
<https://doi.org/10.1126/science.1118435>
- Fleck, D., Mundt, N., Bruentgens, F., Geilenkirchen, P., Machado, P. A., Veitinger, T., ... Spehr, M. (2016). Distinct purinergic signaling pathways in prepubescent mouse spermatogonia. *Journal of General Physiology*, *148*(3), 253–271.  
<https://doi.org/10.1085/jgp.201611636>
- Fowler, B. J., Gelfand, B. D., Kim, Y., Kerur, N., Tarallo, V., Hirano, Y., ... Ambati, J. (2014). Nucleoside reverse transcriptase inhibitors possess intrinsic anti-inflammatory activity. *Science*, *346*(6212), 1000–1003. <https://doi.org/10.1126/science.1261754>
- Fredholm, B. B., Ijzerman, A. P., Jacobson, K. A., Klotz, K. N., & Linden, J. (2001). International Union of Pharmacology. XXV. Nomenclature and classification of adenosine receptors. *Pharmacological Reviews*, *53*(4), 527–552.
- Fredholm, Bertil B., Abbracchio, M. P., Burnstock, G., Dubyak, G. R., Harden, T. K., Jacobson, K. A., ... Williams, M. (1997). Towards a revised nomenclature for P1 and P2 receptors. *Trends in Pharmacological Sciences*, *18*(3), 79–82.  
[https://doi.org/10.1016/S0165-6147\(96\)01038-3](https://doi.org/10.1016/S0165-6147(96)01038-3)
- Garcia-Guzman, M., Soto, F., Laube, B., & Stühmer, W. (1996). Molecular cloning and functional expression of a novel rat heart P2X purinoceptor. *FEBS Letters*, *388*(2–3), 123–127. [https://doi.org/10.1016/0014-5793\(96\)00499-1](https://doi.org/10.1016/0014-5793(96)00499-1)
- Garcia-Guzman, M., Stühmer, W., & Soto, F. (1997). Molecular characterization and pharmacological properties of the human P2X3 purinoceptor. *Molecular Brain Research*, *47*(1–2), 59–66. [https://doi.org/10.1016/S0169-328X\(97\)00036-3](https://doi.org/10.1016/S0169-328X(97)00036-3)
- Gever, J. R., Cockayne, D. A., Dillon, M. P., Burnstock, G., & Ford, A. P. D. W. (2006). Pharmacology of P2X channels. *Pflügers Archiv European Journal of Physiology*, *452*(5), 513–537. <https://doi.org/10.1007/s00424-006-0070-9>
- Glass, R., Bardini, M., Robson, T., & Burnstock, G. (2001). Expression of nucleotide P2X receptor subtypes during spermatogenesis in the adult rat testis. *Cells Tissues Organs*, *169*(4), 377–387. <https://doi.org/10.1159/000047905>
- Gonnord, P., Delarasse, C., Auger, R., Benihoud, K., Prigent, M., Cuif, M. H., ...

- Kanellopoulos, J. M. (2009). Palmitoylation of the P2X7 receptor, an ATP-gated channel, controls its expression and association with lipid rafts. *The FASEB Journal*, 23(3), 795–805. <https://doi.org/10.1096/fj.08-114637>
- Gonzales, E. B., Kawate, T., & Gouaux, E. (2009). Pore architecture and ion sites in acid-sensing ion channels and P2X receptors. *Nature*, 460(7255), 599–604. <https://doi.org/10.1038/nature08218>
- Gu, B. J., Rathsam, C., Stokes, L., McGeachie, A. B., & Wiley, J. S. (2009). Extracellular ATP dissociates nonmuscle myosin from P2X7 complex: This dissociation regulates P2X7 pore formation. *American Journal of Physiology - Cell Physiology*, 297(2). <https://doi.org/10.1152/ajpcell.00079.2009>
- Gu, B. J., Saunders, B. M., Jursik, C., & Wiley, J. S. (2010). The P2X7-nonmuscle myosin membrane complex regulates phagocytosis of nonopsonized particles and bacteria by a pathway attenuated by extracellular ATP. *Blood*, 115(8), 1621–1631. <https://doi.org/10.1182/blood-2009-11-251744>
- Gu, B. J., Saunders, B. M., Petrou, S., & Wiley, J. S. (2011). P2X 7 Is a Scavenger Receptor for Apoptotic Cells in the Absence of Its Ligand, Extracellular ATP . *The Journal of Immunology*, 187(5), 2365–2375. <https://doi.org/10.4049/jimmunol.1101178>
- Gu, B. J., & Wiley, J. S. (2018). P2X7 as a scavenger receptor for innate phagocytosis in the brain. *British Journal of Pharmacology*, 175(22), 4195–4208. <https://doi.org/10.1111/bph.14470>
- Haines, W. R., Voigt, M. M., Migita, K., Torres, G. E., & Egan, T. M. (2001). On the contribution of the first transmembrane domain to whole-Cell current through an ATP-gated ionotropic P2X receptor. *Journal of Neuroscience*, 21(16), 5885–5892. <https://doi.org/10.1523/jneurosci.21-16-05885.2001>
- Hattori, M., & Gouaux, E. (2012). Molecular mechanism of ATP binding and ion channel activation in P2X receptors. *Nature*, 485(7397), 207–212. <https://doi.org/10.1038/nature11010>
- Heymann, G., Dai, J., Li, M., Silberberg, S. D., Zhou, H. X., & Swartz, K. J. (2013). Inter- and intrasubunit interactions between transmembrane helices in the open state of P2X receptor channels. *Proceedings of the National Academy of Sciences of the United States of America*, 110(42), 4045–4054. <https://doi.org/10.1073/pnas.1311071110>

- Honore, P., Donnelly-roberts, D., Namovic, M. T., Hsieh, G., Zhu, C. Z., Mikusa, J. P., ... Jarvis, M. F. (2006). A-740003 [N-(1-[(cyanoimino)(5-quinolinylamino)methyl]amino)-2,2-dimethylpropyl)-2-(3,4-dimethoxyphenyl)acetamide], a novel and selective P2X7 receptor antagonist, dose-dependently reduces neuropathic pain in the rat. *The Journal of Pharmacology and Experimental Therapeutics*, 319(3), 1376–1385. <https://doi.org/10.1124/jpet.106.111559>
- Jelínková, I., Vávra, V., Jindrichova, M., Obsil, T., Zemkova, H. W., Zemkova, H., & Stojilkovic, S. S. (2008). Identification of P2X4 receptor transmembrane residues contributing to channel gating and interaction with ivermectin. *Pflugers Archiv European Journal of Physiology*, 456(5), 939–950. <https://doi.org/10.1007/s00424-008-0450-4>
- Kaan, T. K. Y., Yip, P. K., Patel, S., Davies, M., Marchand, F., Cockayne, D. A., ... McMahon, S. B. (2010). Systemic blockade of P2X3 and P2X2/3 receptors attenuates bone cancer pain behaviour in rats. *Brain*, 133(9), 2549–2564. <https://doi.org/10.1093/brain/awq194>
- Kanellopoulos, J. M., Almeida-da-Silva, C. L. C., Rüütel Boudinot, S., & Ojcius, D. M. (2021). Structural and Functional Features of the P2X4 Receptor: An Immunological Perspective. *Frontiers in Immunology*, 12(March), 1–21. <https://doi.org/10.3389/fimmu.2021.645834>
- Karasawa, A., & Kawate, T. (2016). Structural basis for subtype-specific inhibition of the P2X7 receptor. *ELife*, 5. <https://doi.org/10.7554/elife.22153>
- Karasawa, A., Michalski, K., Mikhelzon, P., & Kawate, T. (2017). The P2X7 receptor forms a dye-permeable pore independent of its intracellular domain but dependent on membrane lipid composition. *ELife*, 6(1), 1–22. <https://doi.org/10.7554/eLife.31186>
- Kawate, T., Michel, J. C., Birdsong, W. T., & Gouaux, E. (2009). Crystal structure of the ATP-gated P2X4 ion channel in the closed state. *Nature*, 460(7255), 592–598. <https://doi.org/10.1038/nature08198>
- Khakh, B. S., & Alan North, R. (2006). P2X receptors as cell-surface ATP sensors in health and disease. *Nature*, 442(7102), 527–532. <https://doi.org/10.1038/nature04886>
- Khakh, B. S., Buenstock, G., Kennedy, C., King, B. F., North, R. A., Séguéla, P., ... Humphrey, P. P. A. (2001). International union of pharmacology. XXIV. Current status of the nomenclature and properties of P2X receptors and their subunits. *Pharmacological*

*Reviews*, 53(1), 107–118.

- Khakh, B. S., Proctor, W. R., Dunwiddie, T. V, Labarca, C., & Lester, H. A. (1999). Allosteric Control of Gating and Kinetics at P2X4 Receptor Channels. *The Journal of Neuroscience*, 19(17), 7289–7299.
- Khmyz, V., Maximyuk, O., Teslenko, V., Verkhatsky, A., & Krishtal, O. (2008). P2X3 receptor gating near normal body temperature. *Pflugers Archiv European Journal of Physiology*, 456(2), 339–347. <https://doi.org/10.1007/s00424-007-0376-2>
- Kim, M., Jiang, L., Wilson, H. L., North, R. A., & Surprenant, A. (2001). Proteomic and functional evidence for a P2X7 receptor signalling complex. *EMBO Journal*, 20(22), 6347–6358.
- King, B. F., Townsend-Nicholson, A., Swildman, S., Thomas, T., Spyer, K. M., & Burnstock, G. (2000). Coexpression of rat P2X2 and P2X6 subunits in *Xenopus* oocytes. *Journal of Neuroscience*, 20(13), 4871–4877. <https://doi.org/10.1523/jneurosci.20-13-04871.2000>
- Kopp, R., Krautloher, A., Ramírez-Fernández, A., & Nicke, A. (2019). P2X7 Interactions and Signaling – Making Head or Tail of It. *Frontiers in Molecular Neuroscience*, 12(August), 1–25. <https://doi.org/10.3389/fnmol.2019.00183>
- Kozik, P., Francis, R. W., Seaman, M. N. J., & Robinson, M. S. (2010). A Screen for Endocytic Motifs. *Traffic*, 11(6), 843–855. <https://doi.org/10.1111/j.1600-0854.2010.01056.x>
- Krůšek, J., & Zemková, H. (1994). Effect of ivermectin on  $\gamma$ -aminobutyric acid-induced chloride currents in mouse hippocampal embryonic neurones. *European Journal of Pharmacology*, 259(2), 121–128. [https://doi.org/10.1016/0014-2999\(94\)90500-2](https://doi.org/10.1016/0014-2999(94)90500-2)
- Lazarowski, E. R., Boucher, R. C., & Harden, T. K. (2003). Mechanisms of release of nucleotides and integration of their action as P2X- and P2Y-receptor activating molecules. *Molecular Pharmacology*, 64(4), 785–795. <https://doi.org/10.1124/mol.64.4.785>
- Lê, K. T., Babinski, K., & Séguéla, P. (1998). Central P2X4 and P2X6 channel subunits coassemble into a novel heteromeric ATP receptor. *Journal of Neuroscience*, 18(18), 7152–7159. <https://doi.org/10.1523/jneurosci.18-18-07152.1998>
- Lê, K. T., Boué-Grabot, E. É., Archambault, V., & Séguéla, P. (1999). Functional and

- biochemical evidence for heteromeric ATP-gated channels composed of P2X1 and P2X5 subunits. *Journal of Biological Chemistry*, 274(22), 15415–15419.  
<https://doi.org/10.1074/jbc.274.22.15415>
- Lecut, C., Frederix, K., Johnson, D. M., Deroanne, C., Thiry, M., Faccinetto, C., ... Oury, C. (2009). P2X 1 Ion Channels Promote Neutrophil Chemotaxis through Rho Kinase Activation . *The Journal of Immunology*, 183(4), 2801–2809.  
<https://doi.org/10.4049/jimmunol.0804007>
- Leduc-Pessah, H., Weiling, N. L., Fan, C. Y., Burma, N. E., Thompson, R. J., & Trang, T. (2017). Site-specific regulation of P2X7 receptor function in microglia gates morphine analgesic tolerance. *Journal of Neuroscience*, 37(42), 10154–10172.  
<https://doi.org/10.1523/JNEUROSCI.0852-17.2017>
- Leonzino, M., Reinisch, K. M., & De Camilli, P. (2021). Insights into VPS13 properties and function reveal a new mechanism of eukaryotic lipid transport. *Biochimica et Biophysica Acta - Molecular and Cell Biology of Lipids*, 1866(10), 159003.  
<https://doi.org/10.1016/j.bbalip.2021.159003>
- Li, Z., Migita, K., Samways, D. S. K., Voigt, M. M., & Egan, T. M. (2004). Gain and loss of channel function by alanine substitutions in the transmembrane segments of the rat ATP-gated P2X2 receptor. *Journal of Neuroscience*, 24(33), 7378–7386.  
<https://doi.org/10.1523/JNEUROSCI.1423-04.2004>
- Libert, F., Parmentier, M., Lefort, A., Dinsart, C., Van Sande, J., Maenhaut, C., ... Vassart, G. (1989). Selective amplification and cloning of four new members of the G protein-coupled receptor family. *Science*, 244(4904), 569–572.  
<https://doi.org/10.1126/science.2541503>
- Luo, J., Yin, G. F., Gu, Y. Z., Liu, Y., Dai, J. P., Li, C., & Li, Z. W. (2006). Characterization of three types of ATP-activated current in relation to P2X subunits in rat trigeminal ganglion neurons. *Brain Research*, 1115(1), 9–15.  
<https://doi.org/10.1016/j.brainres.2006.07.084>
- Luria, A., Rubinstein, S., Lax, Y., & Breitbart, H. (2002). Extracellular adenosine triphosphate stimulates acrosomal exocytosis in bovine spermatozoa via P2 purinoceptor. *Biology of Reproduction*, 66(2), 429–437. <https://doi.org/10.1095/biolreprod66.2.429>
- Lynch, K. J., Touma, E., Niforatos, W., Kage, K. L., Burgard, E. C., Van Biesen, T., ...

- Jarvis, M. F. (1999). Molecular and functional characterization of human P2X2 receptors. *Molecular Pharmacology*, *56*(6), 1171–1181.  
<https://doi.org/10.1124/mol.56.6.1171>
- Mansoor, S. E., Lü, W., Oosterheert, W., Shekhar, M., Tajkhorshid, E., & Gouaux, E. (2016). X-ray structures define human P2X<sub>3</sub> receptor gating cycle and antagonist action. *Nature*, *538*(7623), 66–71. <https://doi.org/10.1038/nature19367>
- Marie Jindrichova, Vojtech Vavra, Tomas Obsil, Stanko S. Stojilkovic, and H., & Zemkova. (2010). Functional relevance of aromatic residues in the first transmembrane domain of P2X receptors. *J Neurochem*, *109*(3), 923–934.
- McCarthy, A. E., Yoshioka, C., & Mansoor, S. E. (2019). Full-Length P2X<sub>7</sub> Structures Reveal How Palmitoylation Prevents Channel Desensitization. *Cell*, *179*(3), 659–670.e13. <https://doi.org/10.1016/j.cell.2019.09.017>
- Michel, A. D., Chambers, L. J., Clay, W. C., Condreay, J. P., Walter, D. S., & Chessell, I. P. (2007). Direct labelling of the human P2X<sub>7</sub> receptor and identification of positive and negative cooperativity of binding. *British Journal of Pharmacology*, *151*(1), 84–95.  
<https://doi.org/10.1038/sj.bjp.0707196>
- Michel, A. D., Chambers, L. J., & Walter, D. S. (2008). Negative and positive allosteric modulators of the P2X<sub>7</sub> receptor. *British Journal of Pharmacology*, *153*(4), 737–750.  
<https://doi.org/10.1038/sj.bjp.0707625>
- Michel, A. D., Clay, W. C., Ng, S. W., Roman, S., Thompson, K., Condreay, J. P., ... Senger, S. (2008). Identification of regions of the P2X<sub>7</sub> receptor that contribute to human and rat species differences in antagonist effects. *British Journal of Pharmacology*, *155*(5), 738–751. <https://doi.org/10.1038/bjp.2008.306>
- Miklavc, P., Thompson, K. E., & Frick, M. (2013). A new role for P2X<sub>4</sub> receptors as modulators of lung surfactant secretion. *Frontiers in Cellular Neuroscience*, *7*(OCT).  
<https://doi.org/10.3389/fncel.2013.00171>
- Montilla, A., Mata, G. P., Matute, C., & Domercq, M. (2020). Contribution of p2x4 receptors to cns function and pathophysiology. *International Journal of Molecular Sciences*, *21*(15), 1–16. <https://doi.org/10.3390/ijms21155562>
- Moura, G. E. D. D., Lucena, S. V., Lima, M. A., Nascimento, F. D., Gesteira, T. F., Nader, H.

- B., ... Tersariol, I. L. S. (2015). P2X7 receptor activity regulation: The role of CD44 proteoglycan GAG chains. *Cell Death and Disease*, 6(11), 6–7.  
<https://doi.org/10.1038/cddis.2015.340>
- Mundt, N., Kenzler, L., & Spehr, M. (2022). Purinergic Signaling in Spermatogenesis. *Frontiers in Endocrinology*, 13(April), 1–7. <https://doi.org/10.3389/fendo.2022.867011>
- Murrell-Lagnado, R. D. (2017). Regulation of P2X Purinergic Receptor Signaling by Cholesterol. In *Current Topics in Membranes* (1st ed., Vol. 80).  
<https://doi.org/10.1016/bs.ctm.2017.05.004>
- Murrell-Lagnado, R. D. (2018). A role for P2X4 receptors in lysosome function. *Journal of General Physiology*, 150(2), 185–187. <https://doi.org/10.1085/jgp.201711963>
- Nicke, A., Bäumer, H. G., Rettinger, J., Eichele, A., Lambrecht, G., Mutschler, E., & Schmalzing, G. (1998). P2X1 and P2X3 receptors form stable trimers: A novel structural motif of ligand-gated ion channels. *EMBO Journal*, 17(11), 3016–3028.  
<https://doi.org/10.1093/emboj/17.11.3016>
- Niemi, K., Teirilä, L., Lappalainen, J., Rajamäki, K., Baumann, M. H., Öörni, K., ... Eklund, K. K. (2011). Serum Amyloid A Activates the NLRP3 Inflammasome via P2X 7 Receptor and a Cathepsin B-Sensitive Pathway . *The Journal of Immunology*, 186(11), 6119–6128. <https://doi.org/10.4049/jimmunol.1002843>
- Niimi, A., Saito, J., Kamei, T., Shinkai, M., Ishihara, H., Machida, M., & Miyazaki, S. (2022). Randomised trial of the P2X3 receptor antagonist sivopixant for refractory chronic cough. *European Respiratory Journal*, 59(6).  
<https://doi.org/10.1183/13993003.00725-2021>
- Nörenberg, W., Sobottka, H., Hempel, C., Plötz, T., Fischer, W., Schmalzing, G., & Schaefer, M. (2012). Positive allosteric modulation by ivermectin of human but not murine P2X7 receptors. *British Journal of Pharmacology*, 167(1), 48–66.  
<https://doi.org/10.1111/j.1476-5381.2012.01987.x>
- North, R. A. (2002). Molecular physiology of P2X receptors. *Physiological Reviews*, 82(4), 1013–1067. <https://doi.org/10.1152/physrev.00015.2002>
- North, R. A. (2004). P2X3 receptors and peripheral pain mechanisms. *Journal of Physiology*, 554(2), 301–308. <https://doi.org/10.1113/jphysiol.2003.048587>

- Ou, A., Gu, B. J., & Wiley, J. S. (2018). The scavenger activity of the human P2X7 receptor differs from P2X7 pore function by insensitivity to antagonists, genetic variation and sodium concentration: Relevance to inflammatory brain diseases. *Biochimica et Biophysica Acta - Molecular Basis of Disease*, 1864(4), 1051–1059. <https://doi.org/10.1016/j.bbadis.2018.01.012>
- Oury, C., & Wéra, O. (2021). P2X1: a unique platelet receptor with a key role in thromboinflammation. *Platelets*, 32(7), 902–908. <https://doi.org/10.1080/09537104.2021.1902972>
- Pankratov, Y., Lalo, U., Verkhatsky, A., & North, R. A. (2006). Vesicular release of ATP at central synapses. *Pflugers Archiv European Journal of Physiology*, 452(5), 589–597. <https://doi.org/10.1007/s00424-006-0061-x>
- Pippel, A., Stolz, M., Woltersdorf, R., Kless, A., Schmalzing, G., & Markwardt, F. (2017). Localization of the gate and selectivity filter of the full-length P2X7 receptor. *Proceedings of the National Academy of Sciences of the United States of America*, 114(11), E2156–E2165. <https://doi.org/10.1073/pnas.1610414114>
- Rettinger, J., & Schmalzing, G. (2004). Desensitization Masks Nanomolar Potency of ATP for the P2X1 Receptor. *Journal of Biological Chemistry*, 279(8), 6426–6433. <https://doi.org/10.1074/jbc.M306987200>
- Riedel, T., Schmalzing, G., & Markwardt, F. (2007). Influence of extracellular monovalent cations on pore and gating properties of P2X7 receptor-operated single-channel currents. *Biophysical Journal*, 93(3), 846–858. <https://doi.org/10.1529/biophysj.106.103614>
- Robinson, L. E., Shridar, M., Smith, P., & Murrell-Lagnado, R. D. (2014a). Plasma membrane cholesterol as a regulator of human and rodent P2X7 receptor activation and sensitization. *Journal of Biological Chemistry*, 289(46), 31983–31994. <https://doi.org/10.1074/jbc.M114.574699>
- Robinson, L. E., Shridar, M., Smith, P., & Murrell-Lagnado, R. D. (2014b). Plasma membrane cholesterol as a regulator of human and rodent P2X7 receptor activation and sensitization. *Journal of Biological Chemistry*, 289(46), 31983–31994. <https://doi.org/10.1074/jbc.M114.574699>
- Roger, S., Pelegrin, P., & Surprenant, A. (2008). Facilitation of P2X7 receptor currents and membrane blebbing via constitutive and dynamic calmodulin binding. *Journal of*

- Neuroscience*, 28(25), 6393–6401. <https://doi.org/10.1523/JNEUROSCI.0696-08.2008>
- Rupert, M., Bhattacharya, A., Sivcev, S., Knezu, M., Cimicka, J., & Zemkova, H. (submitted). Identification of residues in the first transmembrane domain of the rat P2X7 that regulate receptor sensitization and dye uptake function. *Journal of Neurochemistry*.
- Ryoden, Y., Segawa, K., & Nagata, S. (2022). Requirement of Xk and Vps13a for the P2X7-mediated phospholipid scrambling and cell lysis in mouse T cells. *Proceedings of the National Academy of Sciences of the United States of America*, 119(7), 1–9. <https://doi.org/10.1073/pnas.2119286119>
- Sanz, J. M., Chiozzi, P., Ferrari, D., Colaianna, M., Idzko, M., Falzoni, S., ... Di Virgilio, F. (2009). Activation of Microglia by Amyloid  $\beta$  Requires P2X 7 Receptor Expression . *The Journal of Immunology*, 182(7), 4378–4385. <https://doi.org/10.4049/jimmunol.0803612>
- Sarti, A. C., Vultaggio-Poma, V., Falzoni, S., Missiroli, S., Giuliani, A. L., Boldrini, P., ... Di Virgilio, F. (2021). Mitochondrial P2X7 Receptor Localization Modulates Energy Metabolism Enhancing Physical Performance. *Function*, 2(2), 1–15. <https://doi.org/10.1093/function/zqab005>
- Sassenbach, L. (2022). Identification of novel proteins involved in P2X7-mediated signaling cascades. *Purinergic Signalling*, (0123456789), 22–25. <https://doi.org/10.1007/s11302-022-09893-z>
- Sawada, K., Echigo, N., Juge, N., Miyaji, T., Otsuka, M., Omote, H., ... Moriyama, Y. (2008). Identification of a vesicular nucleotide transporter. *Proceedings of the National Academy of Sciences of the United States of America*, 105(15), 5683–5686. <https://doi.org/10.1073/pnas.0800141105>
- Schlegel, R. A., & Williamson, P. (2001). Phosphatidylserine, a death knell. *Cell Death and Differentiation*, 8(6), 551–563. <https://doi.org/10.1038/sj.cdd.4400817>
- Schneider, M., Prudic, K., Pippel, A., Klapperstück, M., Braam, U., Müller, C. E., ... Markwardt, F. (2017). Interaction of purinergic P2X4 and P2X7 receptor subunits. *Frontiers in Pharmacology*, 8(NOV), 1–14. <https://doi.org/10.3389/fphar.2017.00860>
- Schulte, G., & Fredholm, B. B. (2003). Signalling from adenosine receptors to mitogen-activated protein kinases. *Cellular Signalling*, 15(9), 813–827.

[https://doi.org/10.1016/S0898-6568\(03\)00058-5](https://doi.org/10.1016/S0898-6568(03)00058-5)

- Shan, Q., Haddrill, J. L., & Lynch, J. W. (2001). Ivermectin, an Unconventional Agonist of the Glycine Receptor Chloride Channel. *Journal of Biological Chemistry*, 276(16), 12556–12564. <https://doi.org/10.1074/jbc.M011264200>
- Shibuya, I., Tanaka, K., Hattori, Y., Uezono, Y., Harayama, N., Noguchi, J., ... Yamashita, H. (1999). Evidence that multiple P2X purinoceptors are functionally expressed in rat supraoptic neurones. *Journal of Physiology*, 514(2), 351–367. <https://doi.org/10.1111/j.1469-7793.1999.351ae.x>
- Sluyter, R., Shemon, A. N., & Wiley, J. S. (2007). P2X7 receptor activation causes phosphatidylserine exposure in human erythrocytes. *Biochemical and Biophysical Research Communications*, 355(1), 169–173. <https://doi.org/10.1016/j.bbrc.2007.01.124>
- Smart, M. L., Gu, B., Panchal, R. G., Wiley, J., Cromer, B., Williams, D. A., & Petrou, S. (2003). P2X7 receptor cell surface expression and cytolitic pore formation are regulated by a distal C-terminal region. *Journal of Biological Chemistry*, 278(10), 8853–8860. <https://doi.org/10.1074/jbc.M211094200>
- Stoop, R., Surprenant, A., & North, R. A. (1997). Different sensitivities to pH of ATP-induced currents at four cloned P2X receptors. *Journal of Neurophysiology*, 78(4), 1837–1840. <https://doi.org/10.1152/jn.1997.78.4.1837>
- Surprenant, A., Rassendren, F., Kawashima, E., North, R. A., & Buell, G. (1996). The cytolitic P2Z receptor for extracellular ATP identified as a P2X receptor (P2X7). *Science*, 272(5262), 735–738. <https://doi.org/10.1126/science.272.5262.735>
- Suzuki, J., Denning, D. P., Imanishi, E., Horvitz, H. R., & Nagata, S. (2013). Xk-related protein 8 and CED-8 promote phosphatidylserine exposure in apoptotic cells. *Science*, 341(6144), 403–406. <https://doi.org/10.1126/science.1236758>
- Tao, T., Chen, X., Zhou, Y., Zheng, Q., Gao, S., Wang, J., ... Li, W. (2022). Continued P2X7 activation leads to mitochondrial fission and compromising microglial phagocytosis after subarachnoid haemorrhage. *Journal of Neurochemistry*, (September), 419–437. <https://doi.org/10.1111/jnc.15712>
- Teresa Miras-Portugal, P. M., Sebastián-Serrano, Á., De Diego García, L., & Díaz-Hernández, M. (2017). Neuronal P2X7 receptor: Involvement in neuronal physiology

- and. *Journal of Neuroscience*, 37(30), 7063–7072.  
<https://doi.org/10.1523/JNEUROSCI.3104-16.2017>
- Torres-Fuentes, J. L., Rios, M., & Moreno, R. D. (2015). Involvement of a P2X7 Receptor in the Acrosome Reaction Induced by ATP in Rat Spermatozoa. *Journal of Cellular Physiology*, 230(12), 3068–3075. <https://doi.org/10.1002/jcp.25044>
- Vavra, V., Bhattacharya, A., & Zemkova, H. (2011). Facilitation of glutamate and GABA release by P2X receptor activation in supraoptic neurons from freshly isolated rat brain slices. *Neuroscience*, 188, 1–12. <https://doi.org/10.1016/j.neuroscience.2011.04.067>
- Velasquez, S., & Eugenin, E. A. (2014). Role of Pannexin-1 hemichannels and purinergic receptors in the pathogenesis of human diseases. *Frontiers in Physiology*, 5, MAR(March), 1–12. <https://doi.org/10.3389/fphys.2014.00096>
- Vénéreau, E., Ceriotti, C., & Bianchi, M. E. (2015). DAMPs from cell death to new life. *Frontiers in Immunology*, 6(AUG), 1–11. <https://doi.org/10.3389/fimmu.2015.00422>
- Virginio, C., Mackenzie, A., North, R. A., & Surprenant, A. (1999). Kinetics of cell lysis, dye uptake and permeability changes in cells expressing the rat P2X7 receptor. *Journal of Physiology*, 519(2), 335–346. <https://doi.org/10.1111/j.1469-7793.1999.0335m.x>
- Virginio, Caterina, North, R. A., & Surprenant, A. (1998). Calcium permeability and block at homomeric and heteromeric P2X2 and P2X3 receptors, and P2X receptors in rat nodose neurones. *Journal of Physiology*, 510(1), 27–35. <https://doi.org/10.1111/j.1469-7793.1998.027bz.x>
- Virginio, Caterina, Robertson, G., Surprenant, A., & North, R. A. (1998). Trinitrophenyl-substituted nucleotides are potent antagonists selective for P2X1, P2X3, and heteromeric P2X(2/3) receptors. *Molecular Pharmacology*, 53(6), 969–973.
- von Kügelgen, I. (2019). Pharmacology of P2Y receptors. *Brain Research Bulletin*, 151(October 2018), 12–24. <https://doi.org/10.1016/j.brainresbull.2019.03.010>
- Von Kugelgen, I., & Wetter, A. (2000). Molecular pharmacology of P2Y-receptors. *Naunyn-Schmiedeberg's Archives of Pharmacology*, 362(4–5), 310–323.  
<https://doi.org/10.1007/s002100000310>
- Vulchanova, L., Riedl, M. S., Shuster, S. J., Buell, G., Surprenant, A., North, R. A., & Elde, R. (1997). Immunohistochemical study of the P2X2 and P2X3 receptor subunits in rat

- and monkey sensory neurons and their central terminals. *Neuropharmacology*, 36(9), 1229–1242. [https://doi.org/10.1016/S0028-3908\(97\)00126-3](https://doi.org/10.1016/S0028-3908(97)00126-3)
- Wang, W., Hu, D., Feng, Y., Wu, C., Song, Y., Liu, W., ... Wu, J. (2020). Paxillin mediates ATP-induced activation of P2X7 receptor and NLRP3 inflammasome. *BMC Biology*, 18(1), 1–22. <https://doi.org/10.1186/s12915-020-00918-w>
- Watters, J. J., Sommer, J. A., Fisette, P. L., Pfeiffer, Z. A., Aga, M., Prabhu, U., ... Bertics, P. J. (2001). Macrophage Signaling and Mediator Production. *Drug Development Research*, 104, 91–104.
- Wheeler-Schilling, T. H., Marquardt, K., Kohler, K., Guenther, E., & Jabs, R. (2001). Identification of purinergic receptors in retinal ganglion cells. *Molecular Brain Research*, 92(1–2), 177–180. [https://doi.org/10.1016/S0169-328X\(01\)00160-7](https://doi.org/10.1016/S0169-328X(01)00160-7)
- Wildman, S. S., King, B. F., & Burnstock, G. (1999). Modulation of ATP-responses at recombinant rP2X4 receptors by extracellular pH and zinc. *British Journal of Pharmacology*, 126(3), 762–768. <https://doi.org/10.1038/sj.bjp.0702325>
- Wiley, J. S., Sluyter, R., Gu, B. J., Stokes, L., & Fuller, S. J. (2011). The human P2X7 receptor and its role in innate immunity. *Tissue Antigens*, 78(5), 321–332. <https://doi.org/10.1111/j.1399-0039.2011.01780.x>
- Xiong, K., Peoples, R. W., Montgomery, J. P., Chiang, Y., Stewart, R. R., Weight, F. F., & Li, C. (1999). Differential modulation by copper and zinc of P2X2 and P2X4 receptor function. *Journal of Neurophysiology*, 81(5), 2088–2094. <https://doi.org/10.1152/jn.1999.81.5.2088>
- Yan, Z., Khadra, A., Li, S., Tomić, M., Sherman, A., & Stojilkovic, S. S. (2010). Experimental characterization and mathematical modeling of P2X7 receptor channel gating. *Journal of Neuroscience*, 30(42), 14213–14224. <https://doi.org/10.1523/JNEUROSCI.2390-10.2010>
- Yang, D., He, Y., Muñoz-Planillo, R., Liu, Q., & Núñez, G. (2015). Caspase-11 Requires the Pannexin-1 Channel and the Purinergic P2X7 Pore to Mediate Pyroptosis and Endotoxic Shock. *Immunity*, 43(5), 923–932. <https://doi.org/10.1016/j.immuni.2015.10.009>
- Zemkova, H., Tvrdonova, V., Bhattacharya, A., & Jindrichova, M. (2014). Allosteric modulation of ligand gated ion channels by ivermectin. *Physiological Research*,

63(SUPPL.). <https://doi.org/10.33549/physiolres.932711>

Zemkova, Hana, He, M. L., Koshimizu, T. A., & Stojilkovic, S. S. (2004). Identification of ectodomain regions contributing to gating, deactivation, and resensitization of purinergic P2X receptors. *Journal of Neuroscience*, *24*(31), 6968–6978.

<https://doi.org/10.1523/JNEUROSCI.1471-04.2004>

Zhong, Y., Dunn, P. M., Xiang, Z., Bo, X., & Burnstock, G. (1998). Pharmacological and molecular characterization of P2X receptors in rat pelvic ganglion neurons. *British Journal of Pharmacology*, *125*(4), 771–781. <https://doi.org/10.1038/sj.bjp.0702118>

Zhou, Q. Y., Chuanyu, L. I., Olah, M. E., Johnson, R. A., Stiles, G. L., & Civelli, O. (1992). Molecular cloning and characterization of an adenosine receptor: The A3 adenosine receptor. *Proceedings of the National Academy of Sciences of the United States of America*, *89*(16), 7432–7436. <https://doi.org/10.1073/pnas.89.16.7432>